Bioorganic Chemistry 129 (2022) 106144

Contents lists available at ScienceDirect

Bioorganic Chemistry

journal homepage: www.elsevier.com/locate/bioorg

Assessing *p*-tolyloxy-1,3,4-oxadiazole acetamides as lipoxygenase inhibitors assisted by *in vitro* and *in silico* studies

Bushra Bashir [a], Naheed Riaz [a,*], Syeda Abida Ejaz [b], Muhammad Saleem [a], Muhammad Ashraf [a,*], Ambar Iqbal [a,c], Saima Muzaffar [d], Samina Ejaz [c], Aziz-ur-Rehman [e], Hafiz Mohammad Kashif Mahmood [b], Keshab Bhattarai [f]

[a] *Institute of Chemistry, Baghdad-ul-Jadeed Campus, The Islamia University of Bahawalpur, Bahawalpur 63100, Pakistan*
[b] *Department of Pharmaceutical Chemistry, Faculty of Pharmacy, Khawaja Fareed Campus, The Islamia University of Bahawalpur, Bahawalpur 63100, Pakistan*
[c] *Department of Biochemistry, Institute of Biochemistry, Biotechnology and Bioinformatics, Baghdad-ul-Jadeed Campus, The Islamia University of Bahawalpur, Bahawalpur 63100, Pakistan*
[d] *Department of Chemistry, Division of Sceience and Technology, University of Education, 54770, Lahore, Vehari Campus, Pakistan*
[e] *Department of Chemistry, Government College University Lahore, Lahore 54000, Pakistan*
[f] *Department of Pharmaceutical Biology, Auf der Morgenstelle 8, 72076, University of Tuebingen, Tuebingen, Germany*

ARTICLE INFO

Keywords:
Lipoxygenase inhibition
Computational studies
MTT assay
ADME studies
Tolyloxyoxadiazole acetamides
Synthesis
Characterization

ABSTRACT

The underlying correlation between the inflammation, innate immunity and cancer is extensively familiar and linked through a process mediated by three enzymes; cyclooxygenase (COX), lipoxygenase (LOX) and cytochrome P450 (CYP_{450}). The ever increase in the reported side effects of the antiinflammatory drugs against the targeted enzymes and the resistance developed afterwards compels the researchers to synthesize new effective molecules with safer profile. On the basis of these facts, our ongoing research on 1,3,4-oxadiazole derivatives deals with the synthesis of a new series of *N*-alkyl/aralky/aryl derivatives of 5-((*p*-tolyloxymethyl)-4H-1,3,4-oxadiazole-2-ylthio)acetamide (**6a-o**) which were developed by the sequential conversion of *p*-tolyloxyacetic acid (**a**) into ester (**1**) hydrazide (**2**) and 5-(*p*-tolyloxymethyl)-4H-1,3,4-oxadiazole-2-thiol (**3**). The designed compounds (**6a-o**) were acquired by the reaction of 1,3,4-oxadiazole (**3**) with numerous electrophiles (**5a-o**) in KOH. The synthesized analogues (**6a-o**) were characterized by FTIR, ^{1}H-, ^{13}C NMR spectroscopy, EI-MS and HR-EI-MS spectrometry, and were further assessed for their inhibitory potential against the soybean 15-LOX enzyme. The results showed excellent inhibitory potential of the compounds against the said enzyme, specifically **6o, 6b, 6n** and **6e** with inhibitory values ($IC_{50} \pm$ SEM) of 21.5 ± 0.76, 24.3 ± 0.45, 29.1 ± 0.65 and 31.3 ± 0.78 μM, respectively. These compounds displayed < 55 % blood mononuclear cells (MNCs) cellular viability as measured by MTT assay at 0.25 mM concentration. Other compounds demonstrated moderate inhibitory activities with IC_{50} values in the range of 33.2 ± 0.78 to 96.3 ± 0.73 μM and exhibited little cellular viability against MNCs except **6i**, **6j**, **6 m** and **6 k** that showed 61–79 % cellular viability. It was observed that most of the compounds (**6o, 6b, 6n, 6e**) were found more toxic towards MNCs at studied concentration of 0.25 mM. SAR studies revealed that the positions and nature of substituents accompanying phenyl ring have great influence on 15-LOX inhibitory activity. In the most active compound **6o**, the amino acids Asp768 and Val126 were involved in hydrogen bonding, Thr529 was linked with π-anion interaction and π-sulphur interaction was displayed with Tyr525 and two π-alkyl interactions were formed with the benzene ring and amino acid residues Pro530 and Arg533. The *in silico* pharmacokinetics profiles and density functional theory calculations of the compounds further supported the *in vitro* findings. Further work on the synthesis of more oxadiazole derivatives is in progress in search for potential 'leads' for the drug discovery as LOX inhibitors.

* Corresponding authors.
E-mail addresses: nrch322@iub.edu.pk (N. Riaz), abida.ejaz@iub.edu.pk (S. Abida Ejaz), dr.m.ashraf@gmail.com (M. Ashraf), saimarao@ue.edu.pk (S. Muzaffar), samina.ejazsyed@iub.edu.pk (S. Ejaz).

https://doi.org/10.1016/j.bioorg.2022.106144
Received 19 July 2022; Received in revised form 25 August 2022; Accepted 6 September 2022
Available online 11 September 2022

1. Introduction

The discovery of drug leading compounds is a strenuous and usually exorbitant process, which most of them show inadequacy owing to the metabolism and pharmacokinetics impediments instead of potency [1]. Even though inflammation is a common way of fortification and the continual inflammation promote complications with production of intermediates leading to diseases like rheumatoid arthritis, diabetes, atherosclerosis, asthma and cancer. The designing of antiinflammatory agents is of prime requirement to manage such disorders by the two regulatory enzymes pathway: the lipoxygenase (LOX) and cyclooxygenase (COX) pathway [2]. The arachidonic acid (AA) being the substrate for two pathways is one of the major fatty acids required for the maintenance of many physiological functions including tissue regeneration, fluidity and immune response, however, it is reported that its over-consumption plays a vital role in cancer development [3]. AA is produced by phospholipases from the cell membrane, as a response toward a large number of components, which become active during inflammatory situations [4]. The sequence identity between plant and mammalian LOX is found to be 21–27 % as compared to the pair of plant that is 43–86 % while it varies 39–93 % between the pair of mammalian sequences. The 3D orientation of soybean 15-LOXs (L1 and L3) and human 15-LOX-1 and 15-LOX-2 show a high degree of conservation in the catalytic region around the iron atom [5]. The three isomeric COX enzymes, COX-1, COX-2 and COX-3, regulate the COX pathway of inflammation and cancer development. In LOX pathway, 5-LOX, 12-LOX and 15-LOX enzymes produce biologically active leukotrienes and many other molecules [6]. They are also considered major contributors in the production of a wide range of biologically active lipids that take part in inflammation, arachidonic acid metabolism, thrombosis, tumor angiogenesis, the formation of new capillary vessels from existing ones, the substantiation of many physiological processes and the exploitation of various pathological conditions [7]. LOX is present in both plants and animals and is therefore the major target in the discovery of antiinflammatory agents as it plays pivotal role in several types of cancers [8]. Recently, 15-LOX-1 has been described as a target for lowering eoxin production, a pro-inflammatory mediator and a cancer promoter [9]. Currently, the worldwide use of the lipoxygenase inhibitors for medical purposes is getting prominence. So far, 15-LOX inhibitors with different chemical units have been synthesized and classified, including allyl, phenolic, allyloxy benzene and heterocyclic derivatives [10].

Heterocyclic aromatic systems are inexorable in nature, innovative in life sciences as well as in medication. Nitrogen containing heterocyclic compounds especially azole class is attractive in synthesis, as a component of dynamic natural products and in pharmacological and agrochemicals [11]. The transient estimation of the potential pharmacophores manifested that nitrogenous heterocycles are the most common building blocks of small biological molecules as attributed to the stability in human beings because of hydrogen bonding with proteins and nucleic acids [12,13]. The vibrant N—N and C—N bond fused with planar conjugated system therein extends their primacy like high density, excellent stability and top enthalpy of formation [14]. It is reported that oxygenated heterocycles are the second most frequently used heterocycles and seems to be the structural constituent of FDA recommended pharmaceuticals [15]. We are engrossed in such compounds particularly nitrogen and oxygen containing molecules with diverse medicinal and biological applications.

The members of oxadiazole family have extensive applications as electroactive, optoactive and as corrosion inhibitors that reflect their capability to create strong metallic coordination [16,17]. The 1,2,3-, 1,2,4-, 1,2,5- and 1,3,4-oxadiazole isomeric forms arise due to different positions of nitrogen and oxygen in five membered ring [18]. As 1,3,4-oxadiazole isomer has no direct attachment of nitrogen and oxygen atom but developed a crucial pattern for the proliferation of novel drugs with auxiliary activeness to undergo the chemical reactions, have a vast biological importance [19]. Researcher's consideration has been pivotal to 1,2,4- and 1,3,4-oxadiazoles which dominated in medicinal chemistry on account of the sundry prospects of their pharmacological nature including antifungal [20], antibacterial [21], antiviral, antiinflammatory [22], antitumor [23], anti-HIV [24], anticonvulsant, herbicidal [25] and antiproliferative potential [26]. The –N═C–O– group in 1,3,4-oxadiazole core decorates the lipophilicity and this response is its unique pharmacokinetic property that is explored in the discovery of 'lead' molecules [27]. The often used 1,3,4-oxadiazole carrying drugs includes: tiodazosin as an α-1adreneric antagonistic, furamizole as antibacterial, zibotentan as anticancer and ratalgravir as antiretroviral [28] species, along with diverse analogous of oxadiazole with impeccable ability towards metabolic enzymes like carbonic anhydrase [29], butyrylcholinesterase [30], thymidylate synthase [31], α-glucosidase [32,33], aldose reductase [34] and human DNA topoisomerase [35].

The above-mentioned impact of oxadiazole toward enzyme inhibition requires the implementation of innovative compounds comprising a substantial oxadiazole structure which can execute as a stimulant ingredient in the therapeutic field. Following to this idea, we listed a range of series including 1,2,4-triazoles and 1,3,4-oxadiazoles in which a piperidine ring was paired showed powerful 15-LOX inhibitory consequences [7,36–40] and rationalizes our work (Fig. 1).

Our research group is interested in the synthesis of various derivatives and we already published oxadiazoles as LOX inhibitors [43]. In the present study, we synthesized a series of new *N*-alkyl/aralky/aryl oxadiazole derivatives (**6a-o**) and appraised them for their 15-LOX inhibition potential supported by different *in silico* approaches to search new antiinflammatory 'lead' molecules.

2. Results and discussion

2.1. Chemistry

The aspiration of our ongoing study was to synthesize fifteen new 5-(*p*-tolyloxymethyl)-4H-1,3,4-oxadiazole amides (**6a-o**) with a number of substituents and to investigate them for their *in vitro* enzyme inhibition study against 15-LOX assisted by cytotoxicity and *in silico* studies. Syntheses of inter-key molecules as well as the target compounds were acquired by the protocol as shown in Scheme 1. The synthesis was initiated with *p*-tolyloxyacetic acid (**a**), which on reflux using absolute ethanol and further treated with hydrazine hydrate resulted into ester (**1**) first and then hydrazide (**2**), respectively. The ^{1}H NMR spectrum of **2** displayed two singlets at δ 4.04 (1H, –NH) and 8.90 (2H, –NH_2) which represents –$NHNH_2$ scaffold. The hydrazide (**2**) refluxed with CS_2 followed by KOH to obtain intramolecular cyclized product 5-(*p*-tolyloxymethyl)-4H-1,3,4-oxadiazole-2-thiol (**3**). The *N*-alkyl/aralkyl/aryl of 2-bromoacetamides (**5a-o**), is the second unit of target compounds were synthesized by stirring alkyl/aralkyl/aryl amines (**4a-o**; Table 1) with 2-bromoacetyl bromide in a basic medium (pH 9–10). The terminating step was the coalescence of compound **3**, separately with each of the compound of **5a-o** to obtain the target compounds **6a-o**, respectively. This task was performed according to the protocol as given in the experimental section.

The compound **6a** was synthesized as a white amorphous powder. The functional groups were ascertained by infrared (IR) spectrum which showed the absorption bands at 3362, 3030, 2930, 1682, 1658, 1614–1551, 1251 cm^{-1} for N—H, Ar-H, C—H, C═O, C═C, C═N, C—N functionalities, respectively. In ^{1}H NMR spectrum a singlet at δ 2.26 (3H, s, CH_3-Ph) referred to methyl linked with phenyl ring. The spectrum displayed a set of two triplet, and two quatret at δ 1.12 (3H, t, $J = 7.2$ Hz, H-2‴), 1.25 (3H, t, $J = 7.2$ Hz, H-2⁗), 3.31 (2H, q, $J = 7.2$ Hz, H-1‴) and 3.43 (2H, q, $J = 7.2$ Hz, H-1⁗), respectively, nominated the existence of N,*N*-diethyl group. The presences of two proton singlet at δ 5.22 (2H, s, H-5a) stipulates the presence of a methylene attached with oxygen at one end and sp^2-hybridized carbon at other side. In aromatic region the two doublets at δ 6.90 (2H, d, $J = 8.6$ Hz, H-2′,6′) and 7.10 (2H, d, $J = 8.6$ Hz, H-3′,5′) indicated the existent of *p*-substituted phenyl

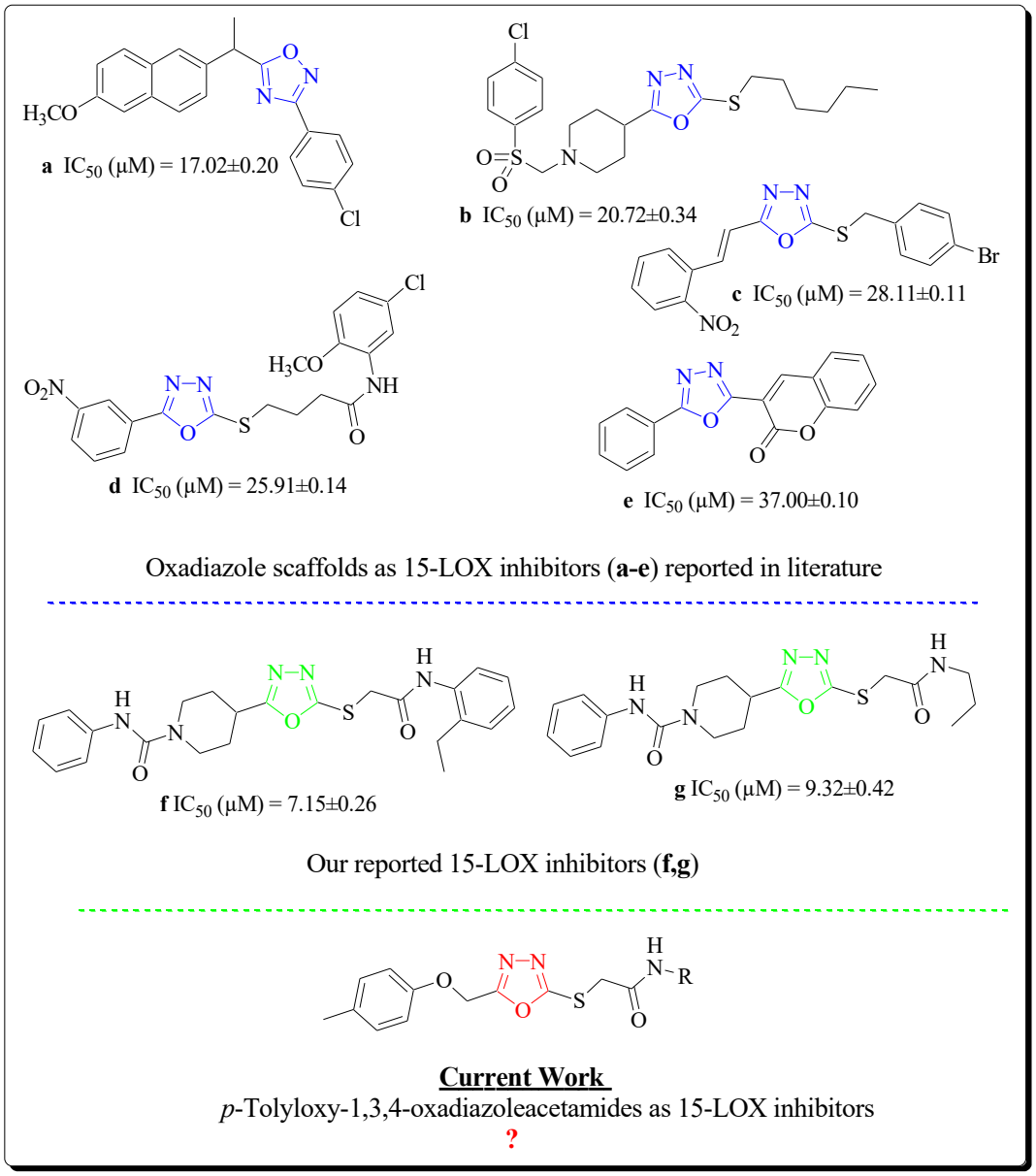

Fig. 1. Rationale of the current research plan and reported LOX inhibitors [7,39–43].

ring. A singlet of two protons at δ 4.38 (2H, s, H-2") designated the methylene linked amide with oxadiazole. The ^{13}C NMR spectra (both BB and DEPT) of **6a** showed total fourteen carbon signals for 16 carbons account for the presence of three methyl, four methylene, four methine and five quaternary carbon atoms. The highly downfield resonances at δ 167.0, 166.9 and 165.2 were imputed to an amide carbonyl and two quaternary carbons of oxadiazole. The signals at δ 115.5, 130.8, 132.4 and 156.6 declared the presence of a *p*-substituted phenyl ring. The signals for two ethyl groups attached to nitrogen atom were observed at δ 13.0, 14.2, 42.0 and 43.7, respectively. The signal generated at δ 20.5 ($\underline{CH_3}$-Ph) declared the presence of a methyl linked with phenyl ring. The signal for methylene group lies between oxygen and sp^2-carbon of oxadiazole appeared at δ 60.7 (C-5a). The molecular formula $C_{16}H_{21}N_3O_3S$ was deduced by using the data of HR-EI-MS which showed the molecular ion $[M]^+$ peak at *m/z* 335.1303 (detailed EI-MS fragmentation pattern is shown in Fig. 2). The spectral data for the remaining compounds **6b-o** of the series is presented in the experimental section.

2.2. LOX inhibitory activities and SAR studies

The current study showed the impact of various substitutions at 1,3,4-oxadiazole family for inhibiting potential of compounds **6a-o** against soybean 15-LOX using quercetin (IC_{50} 4.86 ± 0.14 μM) and baicalein (IC_{50} 2.24 ± 0.13 μM) as standards (Table 2). A number of compounds including **6o, 6b, 6n, 6e** reflected substantial inhibitions (21.5 ± 0.76 to 96.26 ± 0.73 μM) towards the said enzyme (Fig. 3). Even though that the activity is a collaborative property of the entire molecule, for a minimum SAR have been seen owing to anatomize the effectiveness of various alkyl/aralkyl/aryl groups on inhibitory capability as listed below:

i). The compounds **6o** and **6b** showed excellent LOX inhibitory activities with IC_{50} values of 21.5 ± 0.76 and 24.3 ± 0.45 μM, respectively. While assessing the inhibiting potency of **6b** (24.3 ± 0.45 μM) with **6a** (43.8 ± 0.67 μM), it is ascertained that the saturated chain of carbon (*n*-propyl) linked to nitrogen is accountable for its auxiliary activity correlation to four carbons as diethyl groups that combating the binding ability with the enzyme because of its stearic effect.

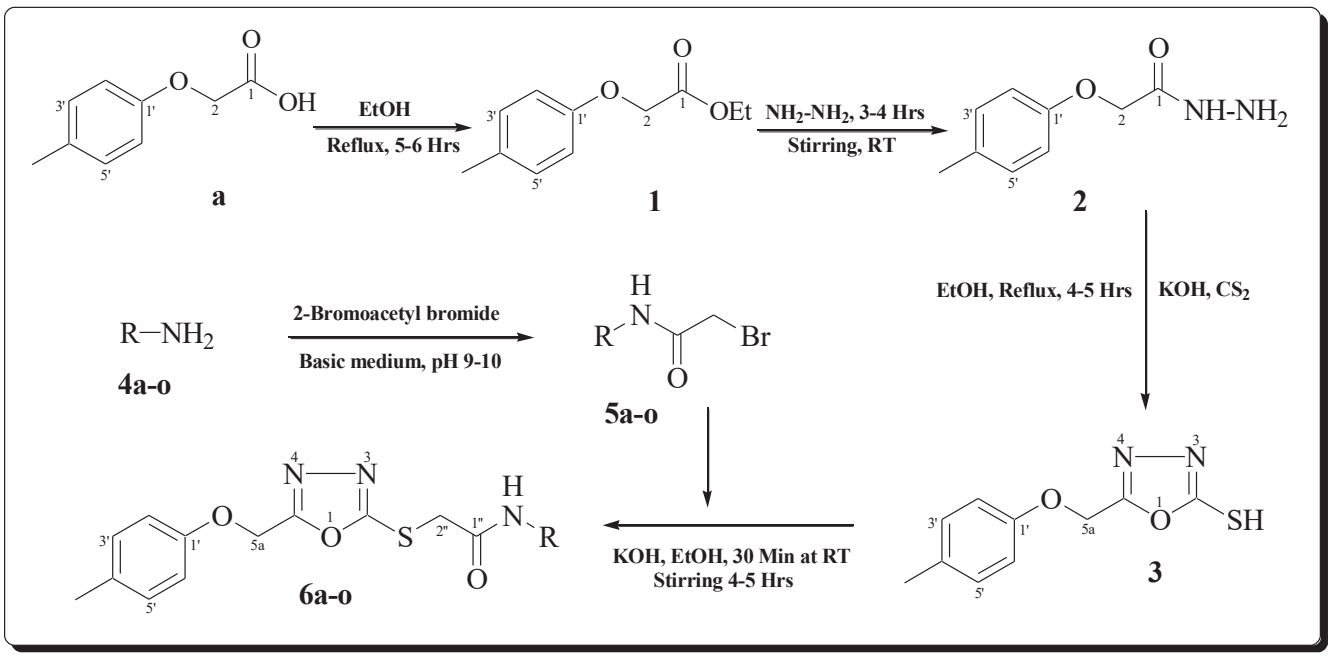

Scheme 1. Schematic representation for the synthesis of oxadiazole amides (**6a-o**) from *p*-tolyloxyacetic acid.

Table 1
Alkyl/aralkyl/aryl substituted amines (**4a-o**).

Comp	R	Comp	R	Comp	R
a	2 x 	**f**	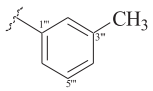	**k**	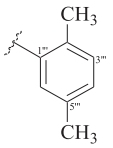
b	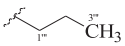	**g**	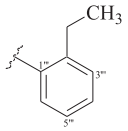	**l**	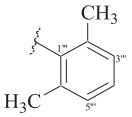
c	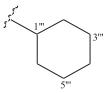	**h**	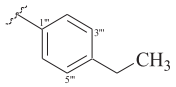	**m**	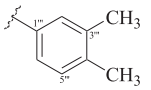
d	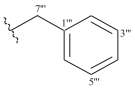	**i**	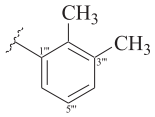	**n**	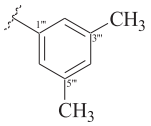
e	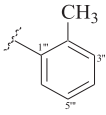	**j**	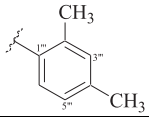	**o**	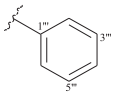

ii). By scrutinizing the activity of **6g** (56.1 ± 0.58 μM) and **6h** (96.3 ± 0.73 μM), the alike substituents (ethyl group) were attached at the *ortho* and *para* positions, respectively, which could be elucidated because of intensive electron donating effect at *ortho* position in aromatic ring impelled the nitrogen to interlink with enzyme that become dilapidated in *para* position supported by the same manner observed for **6e** (31.3 ± 0.78 μM) and **6o** (21.5 ± 0.76 μM).

iii). It is noticed that the electron donating substituents intensified the inhibiting behavior. However, the values found inconsistent in activity due to the position of electron donating groups, and the inhibitory activity becomes lesser where their stearic hindrance is dominated as in **6i** (IC_{50} 78.5 ± 0.85 μM) and **6j** (IC_{50} 57.5 ± 0.67 μM) versus **6l** (IC_{50} 36.3 ± 0.69 μM).

iv). Further, the activity ameliorated by interpolating the unsaturation such as in **6o** (IC_{50} 21.5 ± 0.76 μM) which facilitated the more active positions for inhibiting the enzyme as correlated to **6c** (IC_{50} 33.2 ± 0.78 μM) that lacked unsaturation.

v). The comparable inhibitory potential of **6o** (IC_{50} 21.5 ± 0.76 μM), and **6d** (IC_{50} 79.5 ± 0.69 μM) showed decreased IC_{50} values due to the presence of methylene between nitrogen and phenyl ring that retarded the participation of lone pair of nitrogen with phenyl through resonance.

Therefore, upon looking over the SAR within synthesized derivatives; it may be argued that the positions as well as nature of substituents linked to phenyl ring have great impact on 15-LOX inhibitory

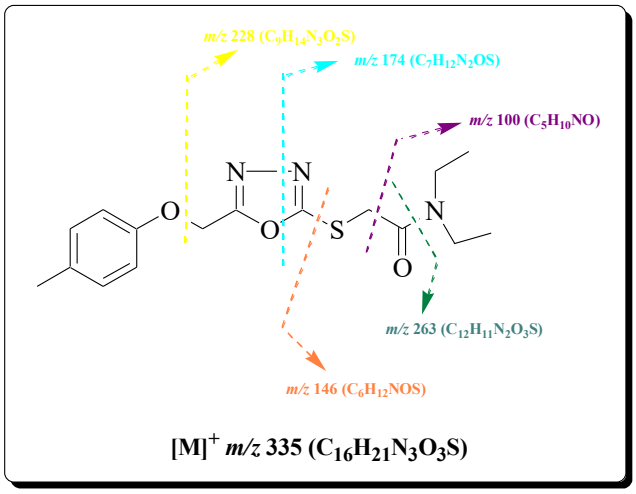

Fig. 2. Plausible EI-MS fragmentation pattern of compound **6a**.

Table 2
15-LOX inhibitory and cytotoxicity profiles of compounds **6a-o** (Mean ± SEM, n = 3).

Comp	Soybean 15-LOX assay		MTT assay
	Inhibition (%) at 0.25 mM	IC_{50} (μM)	Cell viability (%) at 0.25 mM
6a	84.3 ± 1.35	43.8 ± 0.67	32.7 ± 1.6
6b	89.2 ± 1.56	24.3 ± 0.45	45.8 ± 1.7
6c	87.5 ± 1.64	33.2 ± 0.78	47.3 ± 1.6
6d	73.5 ± 1.43	79.5 ± 0.69	38.6 ± 1.4
6e	89.1 ± 1.38	31.3 ± 0.78	28.7 ± 1.3
6f	78.3 ± 1.57	82.5 ± 0.65	34.5 ± 1.8
6g	82.4 ± 1.54	56.1 ± 0.58	23.6 ± 1.5
6h	67.3 ± 1.76	96.3 ± 0.73	41.5 ± 1.4
6i	74.5 ± 1.58	78.5 ± 0.85	79.8 ± 1.7
6j	83.4 ± 1.49	57.5 ± 0.67	68.7 ± 1.5
6k	87.5 ± 1.54	63.4 ± 0.58	61.5 ± 1.6
6l	89.7 ± 1.43	36.3 ± 0.69	43.8 ± 1.2
6m	68.4 ± 1.54	67.6 ± 0.87	63.2 ± 1.5
6n	92.4 ± 1.76	29.1 ± 0.65	37.2 ± 1.4
6o	92.5 ± 1.65	21.5 ± 0.76	54.3 ± 1.8
Quercetin	92.6 ± 1.24	4.86 ± 0.14	Not tested
Baicalein	93.8 ± 1.27	2.24 ± 0.13	Not tested
Cyclophosphamide	–	–	56.5 ± 1.9
Cisplatin	–	–	51.7 ± 1.8
Curcumin	–	–	73.9 ± 1.9

activity.

Cytotoxic studies.

All compounds were tested for their cytotoxicity against human mononuclear cells (MNCs) employing MTT assay at one concentration of 0.25 mM [36–38]. Most of the compounds were toxic to MNCs except **6i**, **6j**, **6m**, **6k** that showed > 61 % cellular viability. Active compounds were found to be toxic to MNCs at this studied concentration. The toxicity towards MNCs increases in the following order of **6i < 6j < 6m < 6k < 6o < 6c < 6b < 6l** and **6g** was found highly toxic. It is speculated that diluted concentrations of these compounds might have lower toxicity profiles around their respective IC_{50} values (Table 2).

2.3. ADME studies

MedChem Designer software ver. 3.0 was used for the prediction of ADME properties (absorption, distribution, metabolism, excretion) which are imperative in the determination of pharmacokinetics properties of molecules and are best expressed in terms of Lipinski's / Veber rule. Accordingly, poor absorption of drug will occur when a ligand has > 5 hydrogen bond donor, molecular weight is > 500, logP > 5 and sum of number of rotatable bonds is >10 and reverse is true for a good molecule [44]. The data (Table 3) shows that all compounds have drug-likeness properties. All molecules have T_PSA < 140 $Å^2$ (topological polar surface area) and represent good oral bioavailability and blood brain barrier penetration property in accordance with the Veber's rule [45]. LogP and logD values represent lipophilicity of molecules; high lipophilic drugs exhibit good properties but too high values decrease its character. Lipophilicity is good indicator and show the drug has good potential to cross cell membrane [46]. In the present studies, most of the compounds exhibited good lipophilicity values except **6a**, **6b**, **6d** and **6o** which showed logP and log D values < 3.0. In summary, these molecules possess the appreciable drug-likeness properties and should be considered for further investigations in search for anti-LOX compounds.

Computational studies.

2.3.1. Molecular docking studies

The molecular operating environment (MOE), 2014.09 software was used for the prediction of the potential active site where the selected ligand can bind and interact within the active pocket of targeted protein, soybean 15-LOX. The binding interactions of the selected compounds along with the controls are shown in Table 4 and as well as in Figs. 4–9.

2.3.2. DFT calculations

In this study, we report the HOMO-LUMO analysis of **6a-o** using DFT/B3LYP calculation setup with basic set 3-21G. The optimized structures of 1,3,4-oxadiazole acetamides (**6a-o**) are given in Fig. 10.

The data shows that **6e** which has the highest energy gap ΔEgap −0.041 tends to be the hardest molecule. Similarly, **6c** has the lowest energy gap ΔEgap −0.267 that allows it to be the softest molecule. The molecule which has the highest HOMO energy is **6g** EHOMO −0.226 turns out to be the best electron donor while the **6k** which has the lowest ELUMO −0.048 value glorifies it to be the best electron acceptor. The best derivative, i.e., **6o** showed the energy gap value −0.26728, and was found stable in quantum chemistry studies. The HOMO-LUMO highest occupied and lowest unoccupied molecular orbitals are very decisive in a molecule. Chemical reactivity of molecule can be determined through HOMO-LUMO band gap. The higher HOMO-LUMO energy band gap, higher will be the kinetic stability, less polarized and lower will be the reactivity and is known as a hard molecule. Similarly, lower the HOMO-LUMO energy band gap, lower will be the stability, more polarized and higher will be the reactivity and is known as a soft molecule (Table 5, Fig. 10,11).

The electrostatic results (Table 4) of the compounds (**6a-o**) and the 15-LOX inhibitory activity (Table 2) displayed the best correlation between the obtained HUMO-LUMO and inhibition studies expressed as IC_{50} values. Briefly, compounds **6o, 6e** and **6a** exhibited LUMO energy of −0.267 eV, −0.267 eV and −0.256 eV, respectively, and also unveiled promising anti-LOX activity. It is suggested that the derivatives with more stabilized LUMO orbitals will have significant LOX activity (Table 5, Fig. 11).

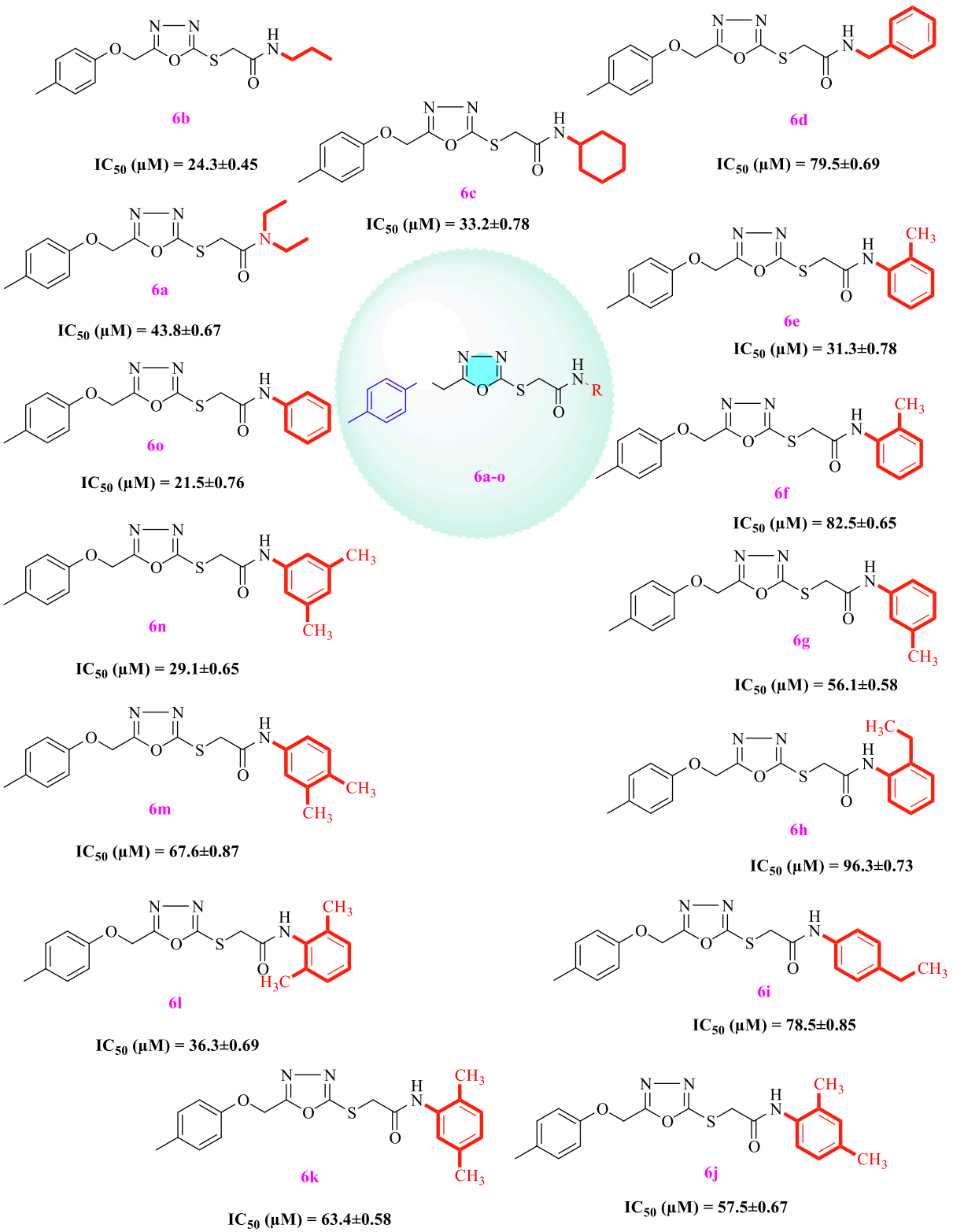

Fig. 3. Compounds as 15-LOX inhibitors of the series **6a-o**.

2.3.3. Global reactivity descriptors

The parameters which are involved in the determination of chemical reactivity include chemical hardness (η), chemical softness (S), electronegativity (X), electrophilicity Index (ω) and electronic chemical potential (μ). The chemical hardness (η = (ELUMO-EHOMO)/2) is represented by reactivity and stability of a chemical system. The electronegativity (X = -(EHOMO + ELUMO) /2) is used to find the power of atom to attract that the electron can be defined as the atom in a molecule which has the power to attract the electrons towards it. Electrophilicity index (ω = μ2 /2η) is a capacity of a molecule to accept electrons using the chemical hardness and electronic chemical potential. The chemical reactivity of the synthesized compounds (**6a-o**) is shown in Table 6.

The Table 5 declares that all the derivatives disclosed low chemical hardness of compounds with the equipotent chemical potential.

Table 3
Calculated ADME properties of compounds **6a-o**.

Comp	Lipophilicity in Moles MlogP	S + logP	S + logD	M. Wt.	No. of rotatable bonds M_NO	Molecular polar surface area T_PSA	No. of hydrogen bond donors HBDH	No. of rule violations
Lipinski / Veber rule	≤ 5	≤ 5	≤ 5	≤ 500	≤ 10	≤ 140 Å^2	≤ 5	< 1
6a	1.722	2.385	2.385	335.427	6	48.46	0	0
6b	1.472	2.152	2.152	321.400	6	77.25	1	0
6c	2.203	3.045	3.045	361.465	6	77.25	1	0
6d	2.202	2.702	2.702	369.445	6	77.25	1	0
6e	2.470	3.169	3.169	369.445	6	77.25	1	0
6f	2.698	3.205	3.205	369.445	6	77.25	1	0
6g	2.698	3.532	3.532	383.472	6	77.25	1	0
6h	2.698	3.579	3.579	383.472	6	77.25	1	0
6i	2.698	3.494	3.494	383.472	6	77.25	1	0
6j	2.698	3.548	3.548	383.472	6	77.25	1	0
6k	3.202	4.094	4.093	399.536	6	68.02	1	0
6l	2.698	3.489	3.489	383.472	6	77.25	1	0
6m	2.698	3.558	3.558	383.472	6	77.25	1	0
6n	2.698	3.599	3.599	383.472	6	77.25	1	0
6o	2.698	2.851	2.850	355.418	6	77.25	1	0
Quercetin	−0.235	1.958	1.529	302.242	7	131.36	5	0
Baicalein	1.296	3.019	2.823	270.243	5	90.90	3	0
Cyclophosphamide	1.966	0.772	0.772	261.089	4	41.57	1	0
Cisplatin	−1.053	1.481	1.481	298.041	2	52.04	4	0
Curcumin	2.256	2.994	2.943	368.389	6	93.06	2	0

Moreover, the compounds **6o, 6b, 6n, 6e, 6c, 6l, 6a, 6g** and **6j** represented a series of comparatively soft molecules with the high polarizability than other compounds of this series, i.e., **6k, 6m, 6i, 6d, 6f** and **6h**. The comparable electronegativity electrophilicity properties of the ligands were also similar and in correlation to the *in vitro* biological data.

3. Conclusions

In conclusion, a series of 5-((*p*-tolyloxymethyl)-4H-1,3,4-oxadiazole-2-ylthio)acetamide core (**6a-o**) were designed, synthesized, characterized and investigated for inhibition studies against 15-LOX. Compounds revealed excellent to moderate inhibiting profiles in the following order of inhibition as **6o > 6b > 6n > 6e > 6c > 6l > 6a > 6g > 6j > 6k > 6m > 6i > 6d > 6f > 6h.** Most of the compounds were toxic towards MNCs at the higher tested concentration of 0.25 mM. SAR studies revealed that the positions as well as nature of substituents linked to phenyl ring of amide side had great impact on 15-LOX inhibitory parameters. Furthermore, the DFT results of the compounds were correlated with the LOX inhibitory activities. The molecular docking results further strengthened the experimental results and the ADME properties exhibited the 'drug-like' properties of the molecules. The work is continued on further derivatization of active compounds in search for more 'lead' compounds as 15-LOX inhibitors.

4. Experimental

4.1. Materials

The required chemical precursors and solvents of analytical rank were procured from local broker of Sigma, Aldrich and Alfa Aesar. The ^{1}H- and ^{13}C NMR spectra were recorded on Bruker instrument operating at 400 and 100 MHz, respectively, using tetramethylsilane as internal standard. The IR spectra were accomplished on Shimadzu 460 FTIR spectrometer using KBr disk. The mass spectra were approved on JMSA 500 mass spectrometer and JMS H × 110 spectrometer with data system. Melting points were logged by using GallenKemp electro-thermal apparatus.

4.2. Synthesis of ethyl p-tolyloxyacetate (1)

p-Tolyloxyacetic acid (**a**; 10 g) was dissolved in 300 mL ethanol in a 500 mL round bottom flask with further addition of 6 mL of conc sulfuric acid. The mixture was refluxed for 5–6 hrs at 60-70℃. The progress of reaction was monitored by TLC and excess amount of cold water was added after completion of reaction. An oily product of yellowish color of ethyl *p*-tolyloxyacetate (**1**) was obtained at pH 8–9 which maintained by sodium carbonate which was separated by solvent extraction using dichloromethane. The physical and spectroscopic data of **1** is as follow:

Yellowish oil; Yield: 90 %; b.p.: 120–121 °C; IR (KBr ν, cm^{-1}): 3030 (Ar-H), 2953 (C—H), 1752 (C═O), 1611–1522 (Ar-C═C); ^{1}H NMR (400 MHz, $CDCl_3$, ppm): δ 1.22 (3H, t, J = 6.9 Hz, $\underline{CH_3}$-CH_2-O), 2.23 (3H, s, $\underline{CH_3}$-Ph), 4.11 (2H, q, J = 6.9 Hz, CH_3-$\underline{CH_2}$-O), 5.30 (2H, s, H-2), 6.61 (2H, d, J = 8.5 Hz, H-2′,6′), 6.82 (2H, d, J = 8.5 Hz, H-3′,5′); ^{13}C NMR (100 MHz, $CDCl_3$, ppm): δ 14.2 ($\underline{CH_3}$-CH_2-O), 21.2 (CH_3-Ph), 61.5 (CH_3-$\underline{CH_2}$-O), 65.2 (C-2), 114.3 (C-2′,6′), 130.4 (C-3′,5′), 130.5 (C-4′), 155.1 (C-1′), 169.1 (C═O); HR-EI-MS (*m/z*): 194.2270 [M]$^+$ calculated for $C_{11}H_{14}O_3$; 194.2250.

4.3. Synthesis of p-tolyloxyaceto hydrazide (2)

Ethyl *p*-tolyloxyacetate (**1**; 0.05 mol, 9.8 mL) was taken in 100 mL round bottom flask and 35 mL of hydrazine hydrate (80 %) was added slowly along continual stirring at room temperature which further carried out for 3–4 hrs. The white precipitates were appeared on cooling which were filtered, washed with cold water and dried. The physical and spectroscopic data of **2** is as follows:

White amorphous powder; Yield: 98 %; m.p.: 132–133 °C; IR (KBr ν, cm^{-1}): 3392, 3353 (N—H), 3031 (Ar-H), 2951 (C—H), 1673 (C═O), 1610–1511 (Ar-C═C); ^{1}H NMR (400 MHz, $CDCl_3$, ppm): 2.26 (3H, s, CH_3-Ph), 4.04 (1H, –NH), 4.61 (2H, s, H-2), 6.91 (2H, d, J = 8.5 Hz, H-2′,6′), 7.11 (2H, d, J = 8.5 Hz, H-3′,5′), 8.90 (2H, –NH_2); ^{13}C NMR (100 MHz, CD_3OD): δ 21.0 (CH_3-Ph), 66.1 (C-2), 114.3 (C-2′,6′), 130.1 (C-3′,5′), 131.3 (C-4′), 155.3 (C-1′), 169.7 (C═O); HR-EI-MS (*m/z*): 180.0898 [M]$^+$ calculated for $C_9H_{12}N_2O_2$; 180.0868.

4.4. Synthesis of 5-(p-tolyloxymethyl)-4H-1,3,4-oxadiazole-2-thiol (3)

The 2-(*p*-tolyloxyaceto hydrazide (**2**; 0.05 mol, 9.0 g) was dissolved in ethanol (50 mL) in 100 mL round bottom flask and 6 mL (0.1 mol) of carbon disulfide was added followed by the addition of 2.8 g (0.05 mol) of potassium hydroxide and refluxed the mixture for 4–5 h. The contents of the flask were poured in ice cold water and maintained pH 5–6 by

Table 4
A summary of the binding interactions of the selected inhibitors.

Comp	Binding energy (kJ/mol)	Hydrophobic interactions	Hydrogen bond interactions	Other interactions
6o	−8.248	Leu246 (π-alkyl), Arg533 (π-alkyl), Val126 (alkyl), Arg767 (alkyl), Tyr532 (amide-π-stacked)	Pro530 (C—H bond), Asp768 (C—H bond)	Lys526 (π-cation) Val762, Asn769, Tyr525, Val520, Leu521, Asn146, Ala145, Trp772, Thr29, His515, Asp243, Glu244 (Van der waals)
6b	−7.937	Phe143 (π-alkyl), Val520 (π-alkyl), Val762 (alkyl), Pro530 (alkyl)	Lys526 (C—H bond bond)	Arg767 (π-anion), Tyr525 (π-sulphur) Ile142, Leu521, Tyr525, Asn835, Arg533, Asn769, Trp772, Ala145, Cys127 (Van der waals)
6n	−7.324	Pro530 (π-alkyl), Arg767 (alkyl), Pro530 (alkyl), Val762 (alkyl), Arg533 (alkyl)	Val126 (Conventional H bond), Asp768 (C—H bond)	Val126 (π-anion), Asp243, Aer129, Arg182, Arg141, Ile142, Glu165, Phe144, Lys526, Asn835, Asn769, Trp772, Tyr525, Cys127 (Van der waals)
6e	−6.943	Arg767 (π-alkyl), Pro530 (π-alkyl), Val126 (alkyl), Ala145 Amide-π stacked)	Trp772 (C—H bond)	Lys526 (π-cation), Thr529, Tyr525, Asn146, Val520, Cys127, Ser129, Asp243, Arg182, Ile142, Asn128, Arg141, Glu165, Asp768, Asn769 (Van der waals)
Baicalein	−6.338	Val126 (π-alkyl), Val520 (π-alkyl)	Asp243 (Conventional H bond), Asn128 (Conventional H bond), Phe143 (C—H bond)	Trp772, Thr773, Lys526, Asn146, His147, Leu521, Glu165, Ser129, Cys127 (Van der waals)
Quercetin	−6.363	Phe143 (π-π stacked), Val126 (π-alkyl), Val520 (π-alkyl)	Asp243 (Conventional H-bond), Cys127 (Conventional H-bond), Trp772 (Conventional H-bond), Lys526 (Conventional H-bond)	Ser129, Arg182, Ile142, Leu521, Ala145, His147, Asn146, Thr773, Asn128, Tyr525 (Van der waals)

using dilute HCl resulted into white precipitates which were filtered, washed and dried. The physical and spectroscopic data of **3** is as follows:

White powder; Yield: 95 %; m.p.: 182–185 °C; IR (KBr ν, cm^{-1}): 3033 (Ar-H), 2930 (C—H), 1632–1552 (Ar-C═C, C═N); ^{1}H NMR (400 MHz, $CDCl_3$, ppm): δ 2.22 (3H, s, CH_3-Ph), 5.19 (2H, s, H-6), 6.91 (2H, d, J = 8.4 Hz, H-2',6'), 7.12 (2H, d, J = 8.4 Hz, H-3',5'); ^{13}C NMR (100 MHz, CD_3OD): δ 20.0 (CH_3-Ph), 59.2 (C-6), 144.4 (C-2',6'), 129.5 (C-3',5'), 131.4 (C-4'), 155.2 (C-1'), 164.7 (C-5), 164.8 (C-2); HR-EI-MS (m/z): 222.0474 $[M]^+$ calculated for $C_{10}H_{10}N_2O_2S$; 222.0463.

4.5. General procedure for the synthesis of compounds *5a-o*

Computed quantity of alkyl/aralkyl/aryl amines (**4a-o**, 0.01 mol) were taken separately in an Erlenmeyer flask already contained 20 % aqueous sodium carbonate solution to maintain the pH 9–10. The 2-bromoacetyl bromide (0.01 mol) was added drop wise into the flask in 2–5 min with constant/vigorous shaking till the appearance of precipitates followed by further stirring in order to get uniform precipitates for 1–2 h. The solid product was filtered, washed with cold water and dried to get the respective electrophile(s), *N*-alky/aralkyl/aryl substituted-3-bromopropanamides (**5a-o**).

4.6. General method for the synthesis of compounds *6a-o*

In a 50 mL round bottom flask, 0.2 g (0.0009 mol) of compound **3** was dissolved in ethanol and 0.6 mmol, 0.036 g of potassium hydroxide was added, the mixture was stirred for 30 min at room temperature. The electrophiles (**5a-o**) were added slowly and separately to the mixture and further stirrer for 4–5 h. Excess amount of cold water was added and the precipitates of the final products, (**6a-o**) were formed, separately, which were filtered, washed and dried.

4.6.1. 5-((p-Tolyloxymethyl)-4H-1,3,4-oxadiazole-2-ylthio)-N,N-diethylacetamide (*6a*)

White amorphous powder; Yield: 97 %; m.p.: 66-68℃; IR (KBr ν, cm^{-1}): 3362 (N—H), 3030 (Ar-H), 2930 (C—H), 1672 (C═O), 1614–1551 (Ar-C═C, C═N), 1251 (C—N); ^{1}H NMR (400 MHz, CD_3OD): δ 1.12 (3H, t, J = 7.2 Hz, H-2‴), 1.14 (3H, t, J = 7.2 Hz, H-2⁗), 2.26 (3H, s, CH_3-Ph), 3.31 (2H, q, J = 7.2 Hz, H-1‴), 3.43 (2H, q, J = 7.2 Hz, H-1⁗), 4.36 (2H, s, H-2″), 5.22 (2H, s, H-5a), 6.90 (2H, d, J = 8.6 Hz, H-2',6'), 7.10 (2H, d, J = 8.6 Hz, H-3',5'); ^{13}C NMR (100 MHz, CD_3OD): δ 13.0 (C-2‴), 14.2 (C-2⁗), 20.5 (CH_3-Ph), 37.1 (C-2″), 42.0 (C-1‴), 43.7 (C-1⁗), 60.7 (C-5a), 115.5 (C-2',6'), 130.8 (C-3',5'), 132.4 (C-4'), 156.6 (C-1'), 165.2 (C-5), 166.9 (C-2), 167.0 (C-1"); HR-EI-MS (m/z): 335.1320 $[M]^+$ calculated for $C_{16}H_{21}N_3O_3S$; 335.1304.

4.6.2. 5-((p-Tolyloxymethyl)-4H-1,3,4-oxadiazole-2-ylthio)-N-n-propylacetamide (*6b*)

White amorphous powder; Yield: 98 %; m.p.: 127–129 ℃; IR (KBr ν, cm^{-1}): 3360 (N—H), 3031 (Ar-H), 2931 (C—H), 1670 (C═O), 1613–1552 (Ar-C═C, C═N), 1250 (C—N); ^{1}H NMR (400 MHz, CD_3OD):

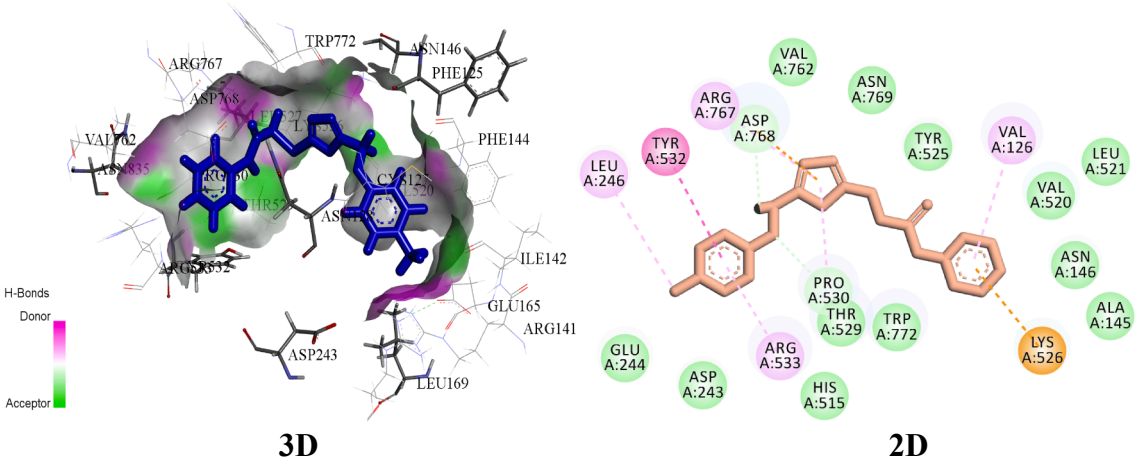

Fig. 4. 3D and 2D binding interactions of **6o** within the active pocket of 15-LOX.

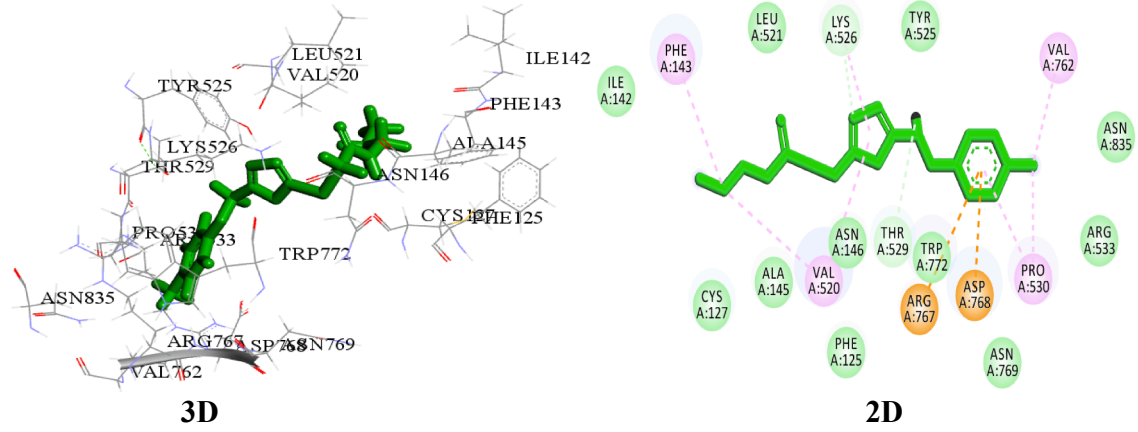

Fig. 5. 3D and 2D binding interactions of **6b** within the active pocket of 15-LOX.

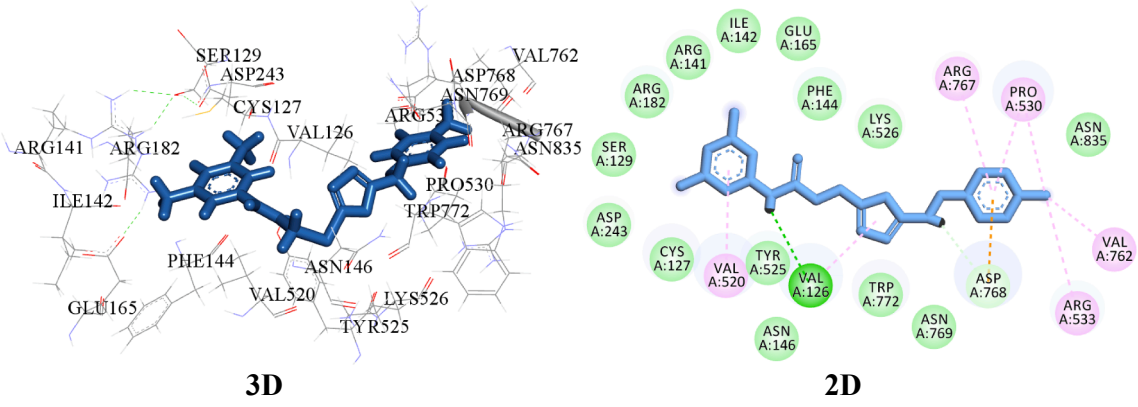

Fig. 6. 3D and 2D binding interactions of **6n** within the active pocket of 15-LOX.

δ 0.87 (3H, t, $J = 7.4$ Hz, H-3‴), 1.48 (2H, sextet, $J = 7.4$ Hz, H-2‴), 2.25 (3H, s, CH_3-Ph), 3.15 (2H, t, $J = 7.4$ Hz, H-1'"), 3.93 (2H, s, H-2"), 5.18 (2H, s, H-5a), 6.87 (2H, d, $J = 8.6$ Hz, H-2',6'), 7.06 (2H, d, $J = 8.6$ Hz, H-3',5'); ^{13}C NMR (100 MHz, CD_3OD): δ 11.4 (C-3‴), 20.5 (CH_3-Ph), 22.7 (C-2'"), 34.0 (C-2"), 42.2 (C-1'"), 60.3 (C-5a), 144.9 (C-2',6'), 130.5 (C-3',5'), 132.1 (C-4'), 155.9 (C-1'), 164.7 (C-5), 166.7 (C-2), 167.7 (C-1"); HR-EI-MS (m/z): 321.1158 $[M]^+$ calculated for $C_{15}H_{19}N_3O_3S$; 321.1148.

*4.6.3. 5-((p-Tolyloxymethyl)-4H-1,3,4-oxadiazole-2-ylthio)-N-cyclohexylacetamide (**6c**)*

White amorphous powder; Yield: 95 %; m.p.:125-128℃; IR (KBr ν, cm^{-1}): 3364 (N—H), 3032 (Ar-H), 2931 (C—H), 1681, 1661 (C═O), 1618–1551 (Ar-C═C, C═N), 1258 (C—N); ^{1}H NMR (400 MHz, CD_3OD): δ 1.13 (2H, m, H-2'"), 1.18 (1H, m, H-4'"), 1.28 (2H, m, H-6'"), 1.65 (1H, m, H-4'"), 1.79 (2H, m, H-3'"), 1.82 (2H, m, H-5'"), 2.27 (3H, s, CH_3-Ph), 3.60 (1H, m, H-1'"), 4.43 (2H, s, H-2"), 5.17 (2H, s, H-5a), 6.84 (2H, d, J

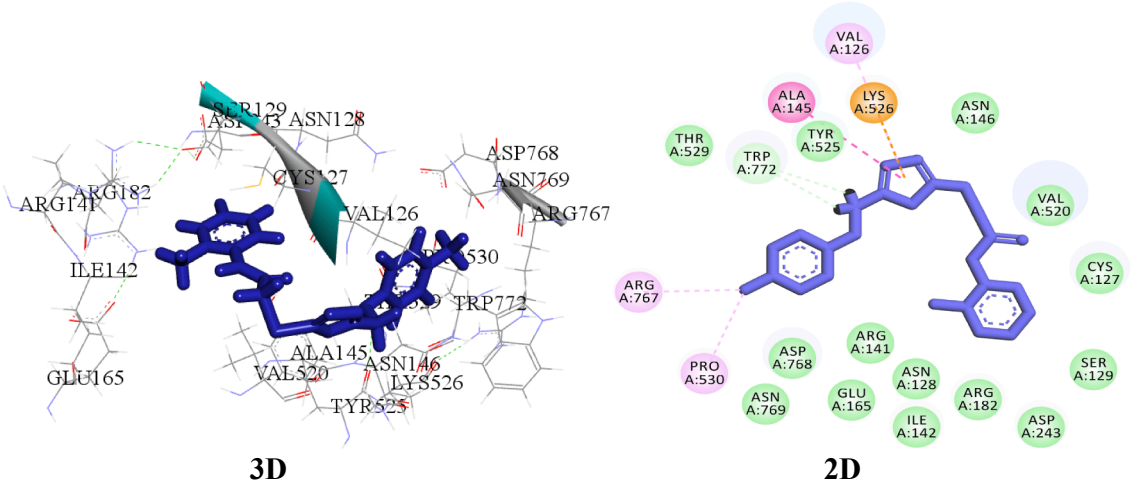

Fig. 7. 3D and 2D binding interactions of **6e** within the active pocket of 15-LOX.

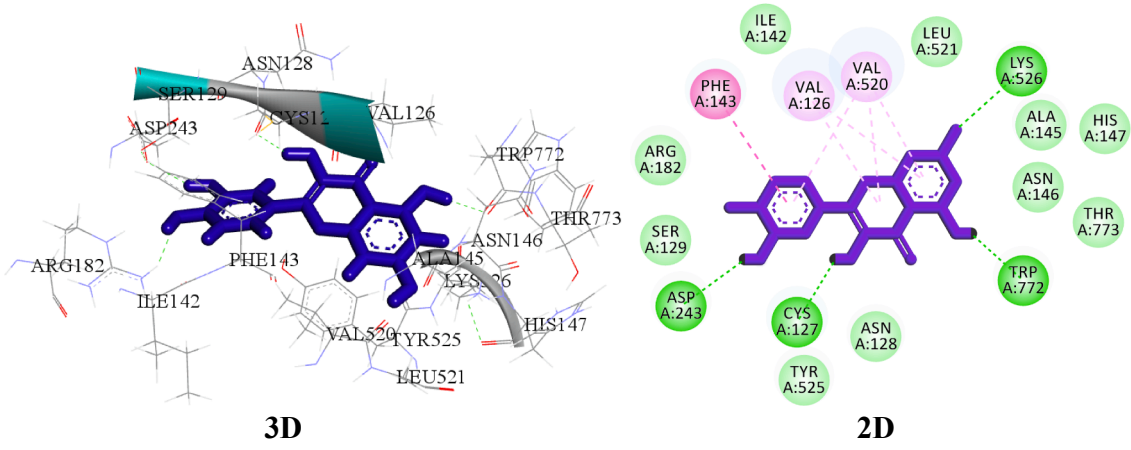

Fig. 8. 3D and 2D binding interactions of the standard (quercetin) within the active pocket of 15-LOX.

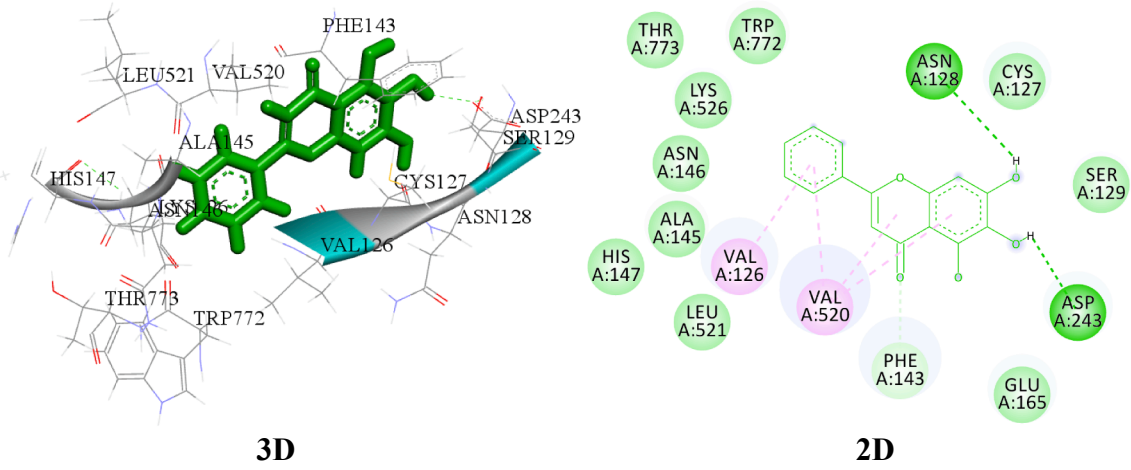

Fig. 9. 3D and 2D binding interactions of standard (baicalein) within the active pocket of 15-LOX.

= 8.2 Hz, H-2',6'), 7.04 (2H, d, J = 8.2 Hz, H-3',5'); ^{13}C NMR (100 MHz, CD_3OD): δ 25.0 (C-2'",6'"), 25.6 (C-4'"), 32.9 (C-3'",5'"), 36.0 (C-2"), 60.1 (C-1'"), 65.6 (C-5a), 114.8 (C-2',6'), 130.4 (C-3',5'), 132.0 (C-4'), 155.6 (C-1'), 164.4 (C-5), 166.4 (C-2), 168.5 (C-1"); HR-EI-MS (m/z): 361.1480 $[M]^+$ calculated for $C_{18}H_{23}N_3O_3S$; 361.1460.

*4.6.4. 5-((p-Tolyloxymethyl)-4H-1,3,4-oxadiazole-2-ylthio)-N-benzylacetamide (**6d**)*

White amorphous powder; Yield: 97 %; m.p.: 137-138C; IR (KBr ν, cm^{-1}): 3342 (N—H), 3031 (Ar-H), 2935 (C—H), 1674 (C═O), 1616–1552 (Ar-C═C, C═N), 1262 (C—N); ^{1}H NMR (400 MHz, CD_3OD):

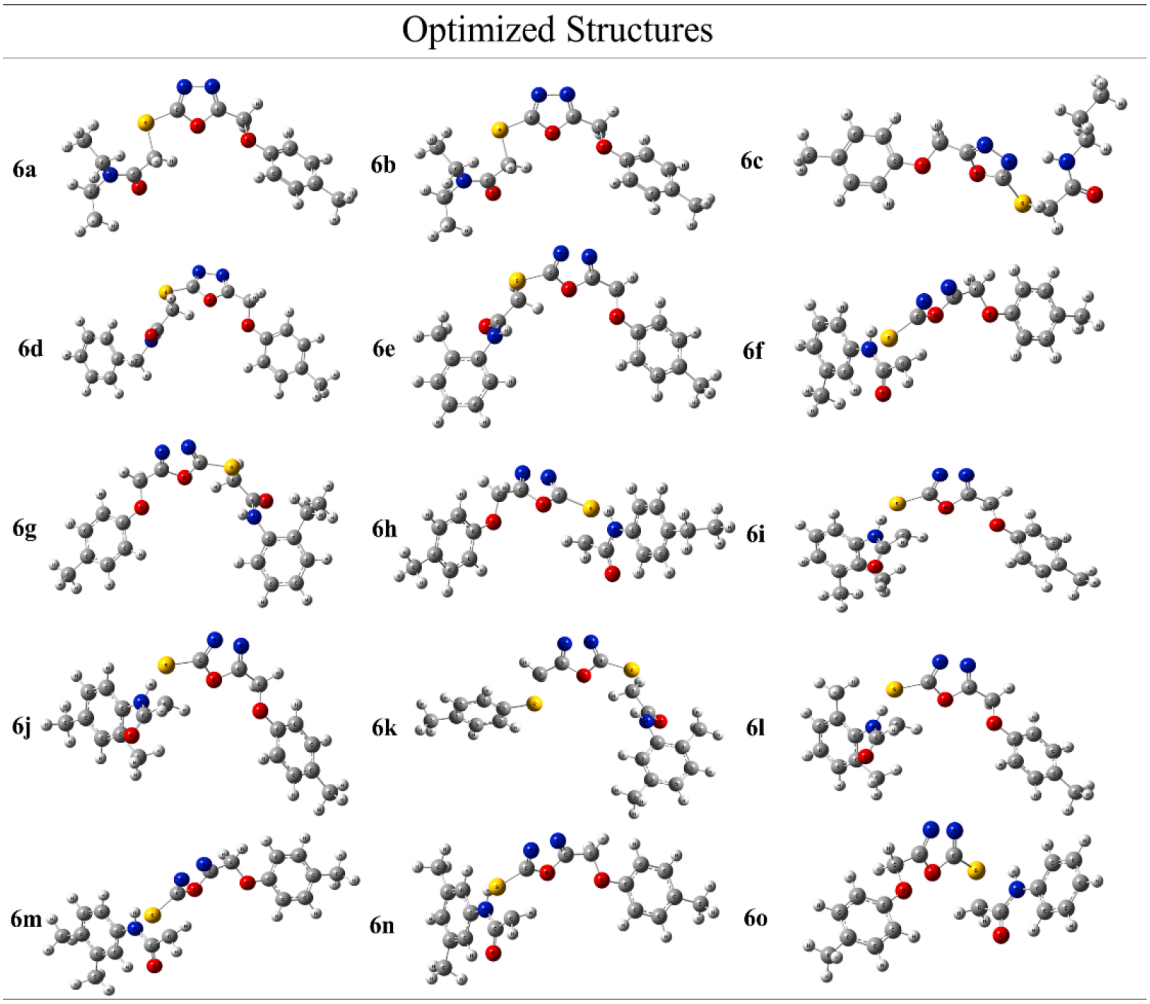

Fig. 10. Optimized structures of **6a-o** using B3LYP/3-21G(d,p) basis set. Red, yellow and blue atoms indicate C, S and O atoms, respectively.

Table 5
Optimization energies, HOMO and LUMO energies and their gap calculated in gas phase.

Comp	Optimization Energy	Dipole moment	HOMO (eV)	LUMO (eV)	Egap (ΔeV)
6a	−1402.889	3.315	−0.221	−0.036	−0.256
6b	−1402.889	3.315	−0.221	−0.034	−0.256
6c	−1363.808	4.760	−0.226	−0.041	−0.041
6d	−1515.373	3.634	−0.225	−0.035	−0.261
6e	−1515.377	3.861	−0.226	−0.041	−0.267
6f	−1515.383	4.336	−0.224	−0.044	−0.268
6g	−1554.478	4.087	−0.226	−0.041	−0.268
6h	−1554.485	4.405	−0.219	−0.043	−0.263
6i	−1554.479	4.742	−0.226	−0.041	−0.267
6j	−1554.481	4.744	−0.226	−0.043	−0.269
6k	−1875.916	5.489	−0.229	−0.048	−0.277
6l	−1554.482	4.410	−0.226	−0.043	−0.269
6m	−1554.487	4.628	−0.216	−0.043	−0.260
6n	−1554.487	4.594	−0.221	−0.043	−0.264
6o	−1476.280	2.501	−0.223	−0.043	−0.267

δ 2.24 (2H, s, CH_3-Ph) 3.39 (2H, s, H-2"), 4.36 (2H, s, H-7'"), 5.11 (2H, s, H-5a), 6.81 (2H, d, J = 8.6 Hz, H-2',6'), 7.06 (2H, d, J = 8.6 Hz, H-3',5'), 7.18–7.27 (5H, m, H-2'"-5'"); ^{13}C NMR (100 MHz, CD_3OD): δ 20.3 (CH_3-Ph), 35.4 (C-2"), 43.8 (C-7'"), 59.7 (C-5a), 114.3 (C-2',6'), 127.3 (2'",6'"), 127.5 (C-4'"), 128.5 (3'",5'"), 130.1 (C-3',5'), 131.7 (C-4'), 137.4 (C-1'"), 155.2 (C-1'), 164.0 (C-5), 165.8 (C-2), 166.8 (C-1"); HR-EI-MS (m/z): 369.1158 $[M]^+$ calculated for $C_{19}H_{19}N_3O_3S$; 369.1148.

*4.6.5. 5-((p-Tolyloxymethyl)-4H-1,3,4-oxadiazole-2-ylthio)-N-2-methylphenylacetamide (**6e**)*

White amorphous powder; Yield: 96 %; m.p.: 130-133℃; IR (KBr ν, cm^{-1}): 3351 (N—H), 3033 (Ar-H), 2931 (C—H), 1671 (C═O), 1615–1553 (Ar-C═C, C═N), 1262 (C—N); ^{1}H NMR (400 MHz, CD_3OD): δ 2.21 (3H, s, CH_3), 2.24 (3H, s, CH_3-Ph), 4.11 (2H, s, H-2"), 5.17 (2H, s, H-5a), 6.84 (2H, d, J = 8.6 Hz, H-2',6'), 7.04 (1H, d, J = 8.6 Hz, H-6'"), 7.06 (2H, d, J = 8.6 Hz, H-3',5'), 7.08 (1H, t, J = 8.4 Hz, H-3'");7.14 (1H, t, J = 8.6 Hz, H-5'"), 7.19 (1H, d, J = 8.4 Hz, H-4'"); ^{13}C NMR (100 MHz, CD_3OD): δ 17.6 (CH_3), 20.4 (CH_3-Ph), 36.2 (C-2"), 60.3 (C-5a), 114.6 (C-2',6'), 124.1 (C-6'"), 126.6 (C-3'"), 127.4 (C-4'"), 130.3 (C-3',5'), 131.3 (C-4'), 131.7 (C-5'"), 131.9 (C-2'"), 135.2 (C-1'"), 155.4 (C-1'), 164.4 (C-5), 166.0 (C-2), 167.6 (C-1"); HR-EI-MS (m/z): 369.1158 $[M]^+$ calculated for $C_{19}H_{19}N_3O_3S$; 369.1148.

*4.6.6. 5-((p-Tolyloxymethyl)-4H-1,3,4-oxadiazole-2-ylthio)-N-3-methylphenylacetamide (**6f**)*

White amorphous powder; Yield: 95 %; m.p.: 120-122℃; IR (KBr ν, cm^{-1}): 3352 (N—H), 3033 (Ar-H), 2934 (C—H), 1673 (C═O), 1619–1556 (Ar-C═C, C═N), 1264 (C—N); ^{1}H NMR (400 MHz, CD_3OD): δ 2.19 (3H, s, CH_3), 2.24 (3H, s, CH_3-Ph), 4.09 (2H, s, H-2"), 5.17 (2H, s, H-5a), 6.84 (2H, d, J = 8.6 Hz, H-2',6'), 6.90 (1H, d, J = 8.6 Hz, H-6'"), 7.04 (2H, d, J = 8.6 Hz, H-3',5'), 7.06 (1H, d, J = 8.6 Hz, H-4'"), 7.29 (1H, t, J = 8.6 Hz, H-5'"), 7.34 (1H, s, H-2'"); ^{13}C NMR (100 MHz, CD_3OD): δ 20.4 (CH_3), 21.4 (CH_3-Ph), 36.8 (C-2"), 60.0 (C-5a), 114.6 (C-2',6'), 117.2 (C-2'"), 120.7 (C-6'"), 125.6 (C-4'"), 128.8 (C-5'"), 130.2 (C-3',5'), 131.3 (C-4'), 137.7 (C-3'"), 138.9 (C-1'"), 155.4 (C-1'), 164.2 (C-5), 166.2

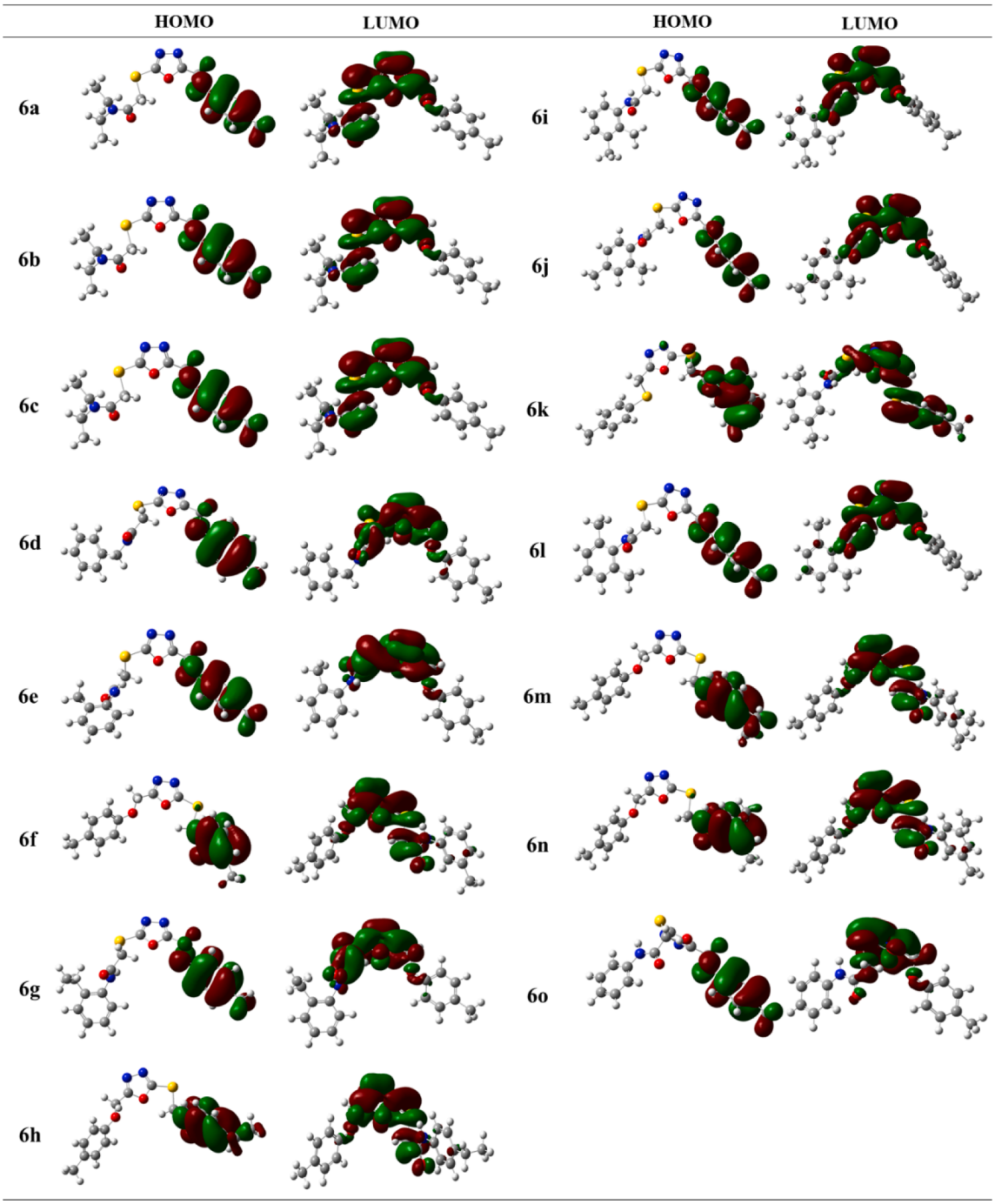

Fig. 11. HOMO-LUMO interfacial plots of the orbitals (**6a-o**). Red, yellow and blue atoms indicate C, S and O atoms, respectively. Deep-red and deep-green parts indicate the different phases of molecular wave functions.

(C-2), 167.0 (C-1"); HR-EI-MS (*m/z*): 369.1158 $[M]^+$ calculated for $C_{19}H_{19}N_3O_3S$; 369.1148.

*4.6.7. 5-((p-Tolyloxymethyl)-4H-1,3,4-oxadiazole-2-ylthio)-N-2-ethylphenylacetamide (**6g**)*

White amorphous powder; Yield: 96 %; m.p.: 128-130℃; IR (KBr ν, cm^{-1}): 3355 (N—H), 3030 (Ar-H), 2932 (C—H), 1676 (C═O), 1618–1553 (Ar-C═C, C═N), 1262 (C—N); ^{1}H NMR (400 MHz, CD_3OD): δ 1.10 (3H, t, J = 7.6 Hz, $\underline{CH_3}$-CH_2), 2.22 (3H, s, CH_3-Ph), 2.53 (2H, q, J = 7.6 Hz, CH_3-$\underline{CH_2}$), 4.06 (2H, s, H-2"), 5.18 (2H, s, H-5a), 6.78 (1H, d, J = 8.6 Hz, H-6'"), 6.84 (2H, d, J = 8.5 Hz, H-2',6'), 7.05 (2H, d, J = 8.5 Hz, H-3',5'), 7.13 (1H, t, J = 8.6 Hz, H-4'"), 7.19 (1H, t, J = 8.6 Hz, H-5'"), 7.51 (1H, d, J = 8.6 Hz, H-3'"); ^{13}C NMR (100 MHz, CD_3OD): δ 14.0 (CH_3), 20.5 (CH_3-Ph), 24.0 (CH_2), 36.2 (C-2"), 60.0 (C-5a), 114.7 (C-2',6'), 125.1 (C-6'"), 126.8 (C-3'"), 127.5 (C-4'"), 128.6 (C-5'"), 129.0 (C-3',5'), 130.3 (C-4'), 134.4 (C-2'"), 137.5 (C-1'"), 155.6 (C-1'), 164.6 (C-5), 166.3 (C-2), 166.5 (C-1"); HR-EI-MS (*m/z*): 383.1314 $[M]^+$ calculated for $C_{20}H_{21}N_3O_3S$; 383.1304.

*4.6.8. 5-((p-Tolyloxymethyl)-4H-1,3,4-oxadiazole-2-ylthio)-N-4-ethylphenylacetamide (**6h**)*

White amorphous powder; Yield: 93 %; m.p.: 157-160℃; IR (KBr ν, cm^{-1}): 3354 (N—H), 3034 (Ar-H), 2935 (C—H), 1677 (C═O), 1612–1555 (Ar-C═C, C═N), 1266 (C—N); ^{1}H NMR (400 MHz, CD_3OD):

Table 6
Global reactivity descriptors for compounds **6a-o**.

Comp	S (eV-1)	X (eV)	μ (eV)	ω (eV)
6a	5.355	0.128	−0.128	0.088
6b	5.355	0.128	−0.128	0.088
6c	5.429	0.133	−0.133	0.097
6d	5.275	0.131	−0.131	0.090
6e	5.408	0.134	−0.134	0.097
6f	5.542	0.134	−0.134	0.100
6g	5.417	0.134	−0.134	0.097
6h	5.672	0.132	−0.132	0.098
6i	5.427	0.134	−0.134	0.097
6j	5.470	0.135	−0.135	0.099
6k	5.528	0.139	−0.139	0.106
6l	5.474	0.135	−0.135	0.100
6m	5.768	0.130	−0.130	0.098
6n	5.646	0.132	−0.132	0.099
6o	5.568	0.134	−0.134	0.099

δ 1.18 (3H, t, J = 7.6 Hz, $\underline{CH_3}$-CH_2), 2.24 (3H, s, CH_3-Ph), 2.58 (2H, q, J = 7.6 Hz, CH_3-$\underline{CH_2}$), 4.10 (2H, s, H-2"), 5.17 (2H, s, H-5a), 6.78 (1H, d, J = 8.6 Hz, H-2'"), 6.85 (1H, d, J = 8.6 Hz, H-6'"), 7.05 (1H, d, J = 8.6 Hz, H-3'"), 7.07(1H, d, J = 8.6 Hz, H5'"), 7.11 (2H, d, J = 8.4 Hz, H-2',6'), 7.41 (2H, d, J = 8.4 Hz, H-3',5'); ^{13}C NMR (100 MHz, CD_3OD): δ 15.5 (CH_3), 20.5 (CH_3-Ph), 31.6 (CH_2), 36.8 (C-2"), 60.1 (C-5a), 114.8 (C-2',6'), 120.4 (C-2'",6'"), 128.5 (C-3'",5'"), 130.2 (C-3',5'), 130.4 (C-4'), 131.4 (C-4'"), 141.3 (C-1'"), 155.6 (C-1'), 164.4 (C-5), 166.2 (C-2), 167.1 (C-1"); HR-EI-MS (*m/z*): 383.1314 [M]$^+$ calculated for $C_{10}H_{21}N_3O_3S$; 383.1304.

*4.6.9. 5-((p-Tolyloxymethyl)-4H-1,3,4-oxadiazole-2-ylthio)-N-2,3-dimethylphenylacetamide **(6i)***

White amorphous powder; Yield: 94 %; m.p.: 156-159℃; IR (KBr ν, cm^{-1}): 3353 (N—H), 3029 (Ar-H), 2934 (C—H), 1672 (C═O), 1614–1556 (Ar-C═C, C═N), 1268 (C—N); ^{1}H NMR (400 MHz, CD_3OD): δ 2.07 (3H, s, CH_3), 2.24 (3H, s, CH_3), 2.25 (3H, s, CH_3-Ph), 4.24 (2H, s, H-2"), 5.18 (2H, s, H-5a), 6.84 (2H, d, J = 8.6 Hz, H-2',6'), 6.99 (1H, d, J = 8.6 Hz, H-6'"), 7.06 (2H, d, J = 8.6 Hz, H-3',5'), 7.18 (1H, d, J = 7.4 Hz, H-4'"), 7.24 (1H, t, J = 8.6 Hz, H-5'"); ^{13}C NMR (100 MHz, CD_3OD): δ 13.9 (CH_3), 20.4 (CH_3), 20.5 (CH_3-Ph), 36.2 (C-2"), 60.1 (C-5a), 114.8 (C-2',6'), 123.1 (C-6'"), 125.9 (C-4'"), 126.9 (C-2'"), 128.3 (C-5'"), 130.2 (C-3',5'), 131.2 (C-4'), 132.0 (C-3'"), 137.9 (C-1'"), 155.5 (C-1'), 164.5 (C-5), 166.3 (C-2), 171.5 (C-1"); HR-EI-MS (*m/z*): 383.1314 [M]$^+$ calculated for $C_{20}H_{21}N_3O_3S$; 383.1304.

*4.6.10. 5-((p-Tolyloxymethyl)-4H-1,3,4-oxadiazole-2-ylthio)-N-2,4-dimethylphenylacetamide **(6j)***

White amorphous powder; Yield: 93 %; m.p.: 129-132℃; IR (KBr ν, cm^{-1}): 3355 (N—H), 3030 (Ar-H), 2934 (C—H), 1673 (C═O), 1618–1558 (Ar-C═C, C═N), 1262 (C—N); ^{1}H NMR (400 MHz, CD_3OD): δ 2.15 (3H, s, CH_3), 2.20 (3H, s, CH_3-Ph), 2.23 (3H,s, CH_3), 4.41 (2H, s, H-2"), 5.18 (2H, s, H-5a), 6.82 (1H, d, J = 8.6 Hz, H-6'"), 6.86 (1H, t, J = 8.6 Hz, H-5'"), 6.95 (2H, d, J = 8.6 Hz, H-2',6'), 7.05 (2H, d, J = 8.6 Hz, H-3',5'), 7.07 (1H, s, H-3'"); ^{13}C NMR (100 MHz, CD_3OD): δ 17.4 (CH_3), 17.8 (CH_3), 20.5 (CH_3-Ph), 36.2 (C-2"), 60.1 (C-5a), 114.8 (C-2',6'), 124.7 (C-3'"), 127.2 (C-6'"), 128.2 (C-2'"), 130.6 (C-3',5'), 131.5 (C-4'), 131.7 (C-5'"), 132.3 (C-4'"), 136.3 (C-1'"), 155.6 (C-1'), 164.6 (C-5), 166.3 (C-2), 171.5 (C-1"); HR-EI-MS (*m/z*): 383.1314 [M]$^+$ calculated for $C_{20}H_{21}N_3O_3S$; 383.1304.

*4.6.11. 5-((p-Tolyloxymethyl)-4H-1,3,4-oxadiazole-2-ylthio)-N-2,5-dimethylphenylacetamide **(6k)***

White amorphous powder; Yield: 96 %; m.p.: 138-141℃; IR (KBr ν, cm^{-1}): 3356 (N—H), 3033 (Ar-H), 2931 (C—H), 1673 (C═O), 1619–1553 (Ar-C═C, C═N), 1263 (C—N); ^{1}H NMR (400 MHz, CD_3OD): δ 2.14 (3H, s, CH_3), 2.23 (3H, s, CH_3-Ph), 2.24 (3H, s, CH_3), 4.51 (2H, s, H-2"), 5.16 (2H, s, H-5a), 6.76 (1H, d, J = 8.6 Hz, H-4'"), 6.84 (2H, d, J = 8.6 Hz, H-2',6'), 7.03 (1H, d, J = 8.6 Hz, H-3'"), 7.07 (2H, d, J = 8.6 Hz, H-3',5'), 7.16 (1H, s, H-6'"); ^{13}C NMR (100 MHz, CD_3OD): δ 17.0 (CH_3), 20.4 (CH_3-Ph), 20.7 (CH_3), 36.1 (C-2"), 59.9 (C-5a), 114.5 (C-2',6'), 124.3 (C-6'"), 128.5 (C-4'"), 130.0 (C-3'"), 130.4 (C-3',5'), 131.1 (C-4'), 131.2 (C-2'"), 131.8 (C-5'"), 136.2 (C-1'"), 155.3 (C-1'), 164.3 (C-5), 166.3 (C-2), 170.1 (C-1"); HR-EI-MS (*m/z*): 383.1314 [M]$^+$ calculated for $C_{20}H_{21}N_3O_3S$; 383.1304.

*4.6.12. 5-((p-Tolyloxymethyl)-4H-1,3,4-oxadiazole-2-ylthio)-N-2,6-dimethylphenylacetamide **(6l)***

White amorphous powder; Yield: 98 %; m.p.: 161-163℃; IR (KBr ν, cm^{-1}): 3356 (N—H), 3034 (Ar-H), 2945 (C—H), 1674 (C═O), 1616–1553 (Ar-C═C, C═N), 1266 (C—N); ^{1}H NMR (400 MHz, CD_3OD): δ 2.16 (3H, s, H-2'"), 2.19 (3H, s, H-6'"), 2.25 (3H, s, CH_3-Ph), 4.19 (2H, s, H-2"), 5.23 (2H, s, H-5a), 6.78 (1H, d, J = 8.6 Hz, H-5'"), 6.84 (2H, d, J = 8.6 Hz, H-2',6'), 7.02 (1H, d, J = 8.6 Hz, H-3'"), 7.05 (2H, d, J = 8.6 Hz, H-3',5'), 7.08 (1H, t, J = 8.6 Hz, H-4'"); ^{13}C NMR (100 MHz, CD_3OD): δ 18.2 (CH_3), 20.5 (CH_3-Ph), 36.0 (C-2"), 60.4 (C-5a), 115.1 (C-2',6'), 128.6 (C-4'"), 129.2 (C-3'",5'"), 130.5 (C-3',5'), 131.6 (C-4'), 134.2 (C-2'",6'"), 136.1 (C-1'"), 156.1 (C-1'), 165.1 (C-5), 166.2 (C-2), 168.4 (C-1"); 383.1314 [M]$^+$ calculated for $C_{20}H_{21}N_3O_3S$; 383.1304.

*4.6.13. 5-((p-Tolyloxymethyl)-4H-1,3,4-oxadiazole-2-ylthio)-N-3,4-dimethylphenylacetamide **(6m)***

White amorphous powder; Yield: 94 %; m.p.: 152-155℃; IR (KBr ν, cm^{-1}): 3356 (N—H), 3034 (Ar–EI-MS (*m/z*): 383.1314 [M]$^+$ calculated H), 2943 (C—H), 1676 (C═O), 1618–1550 (Ar-C═C, C═N), 1265 (C—N); ^{1}H NMR (400 MHz, CD_3OD): δ 2.17 (3H, s, CH_3), 2.19 (3H, s, CH_3), 2.24 (3H, s, CH_3-Ph), 4.09 (2H, s, H-2"), 5.15 (2H, s, H-5a), 6.84 (2H, d, J = 8.5 Hz, H-2',6'), 7.00 (1H, d, J = 8.1 Hz, H-6'"), 7.06 (2H, d, J = 8.5 Hz, H-3',5'), 7.20 (1H, d, J = 8.1 Hz, H-5'"), 7.27 (1H, s, H-2'"); ^{13}C NMR (100 MHz, CD_3OD): δ 19.2 (CH_3), 19.9 (CH_3), 20.5 (CH_3-Ph), 36.9 (C-2"), 60.1 (C-5a), 115.0 (C-2',6'), 117.9 (C-2'"), 121.6 (C-6'"), 130.1 (C-5'"), 130.4 (C-3',5'), 132.0 (C-4'), 133.3 (C-4'"), 135.7 (C-3'"), 137.4 (C-1'"), 155.5 (C-1'), 164.5 (C-5), 165.4 (C-2), 166.2 (C-1"); HR-EI-MS (*m/z*): 383.1314 [M]$^+$ calculated for $C_{20}H_{21}N_3O_3S$; 383.1304.

*4.6.14. 5-((p-Tolyloxymethyl)-4H-1,3,4-oxadiazole-2-ylthio)-N-3,5-dimethylphenylacetamide **(6n)***

White amorphous powder; Yield: 92 %; m.p.: 148-150℃; IR (KBr ν, cm^{-1}): 3350 (N—H), 3032 (Ar-H), 2947 (C—H), 1675 (C═O), 1610–1555 (Ar-C═C, C═N), 1262 (C—N); ^{1}H NMR (400 MHz, CD_3OD): δ 2.30 (6H, s, CH_3), 2.24 (3H, s, CH_3-Ph), 4.10 (2H, s, H-2"), 5.17 (2H, s, H-5a), 6.84 (2H, d, J = 8.6 Hz, H-2',6'), 7.06 (2H, d, J = 8.6 Hz, H-3',5'), 6.73 (1H, s, H-4'"), 7.13 (2H, s, H-2'",6'"); ^{13}C NMR (100 MHz, CD_3OD): δ 20.5 (CH_3-Ph), 21.4 (CH_3), 37.0 (C-2"), 60.2 (C-5a), 115.0 (C-2',6'), 118.1 (C-2'",6'"), 126.7 (C-4'"), 130.3 (C-3',5'), 132.0 (C-4'), 137.9 (C-1'"), 138.8 (C-3'",5'"), 155.7 (C-1'), 164.5 (C-5), 165.6 (C-2), 166.3 (C-1"); HR-EI-MS (*m/z*): 383.1324 [M]$^+$ calculated for $C_{20}H_{21}N_3O_3S$; 383.1304.

*4.6.15. 5-((p-Tolyloxymethyl)-4H-1,3,4-oxadiazole-2-ylthio)-N-phenylacetamide **(6o)***

White amorphous powder; Yield: 92 %; m.p.: 150-153℃; IR (KBr ν, cm^{-1}): 3354 (N—H), 3035 (Ar-H), 2948 (C—H), 1676 (C═O), 1618–1554 (Ar-C═C, C═N), 1265 (C—N); ^{1}H NMR (400 MHz, CD_3OD): δ 2.24 (3H, s, CH_3-Ph), 36.9 (2H, s, H-2"), 5.15 (2H, s, H-5a), 6.84 (2H, d, J = 8.6 Hz, H-2',6'), 7.03 (1H, d, J = 8.4 Hz, H-6'"), 7.05 (1H, d, J = 8.4 Hz, H-2'"), 7.09 (1H, t, J = 8.4 Hz, H-4'"), 7.25 (1H, t, J = 8.4 Hz, H-5'"), 7.28 (1H, t, J = 8.4 Hz, H-3'"), 7.49 (2H, d, J = 8.6 Hz, H-3',5'); ^{13}C NMR (100 MHz, CD_3OD): δ 20.5 (CH_3-Ph), 36.9 (C-2"), 60.1 (C-5a), 114.7 (C-2',6'), 120.2 (C-2'",6'"), 124.8 (C-4'"), 129.1 (C-3'",5'"), 130.3 (C-3',5'), 131.9 (C-4'), 137.9(C-1'"), 155.5 (C-1'), 164.4 (C-5), 165.4 (C-2), 165.9 (C-1"); HR-EI-MS (*m/z* SEM 355.1001 [M]$^+$ calculated for $C_{18}H_{17}N_3O_3S$; 355.0991.

4.7. 15-LOX inhibition assay

The assay was performed according to the chemiluminescence method of Kondo and coworkers [47] with some modifications, as reported earlier [37,43]. Briefly, a total volume of 100 μL of reaction mixture contained 60 μL of borate buffer (200 mM, pH 9.0), 10 μL of test compound or solvent, and 10 μL soybean 15-LOX enzyme. This mixture was incubated at 25℃ in dark for 5 min. Then 10 μL solution of luminol (3 nM) containing cytochrome *c* (1 nM) was added to each well and luminescence was measured by BioTek HTX 96-well plate reader in luminescence mode. The reaction was initiated by the addition of 10 μL linoleic acid substrate solution. Chemiluminescence of the reaction contents was measured for 100 to 300 *sec*. All experiments were performed in triplicates. Quercetin and baicalein were used as positive controls. The percentage of inhibition was calculated using the following formula:

$$\text{Inhibition (\%)} = (\text{Abs of control} - \text{Abs of test comp} / \text{Abs of control}) \times 100$$

The active compounds were suitably diluted and their percentage inhibitions were determined. The obtained data was used for the computation of IC_{50} values using Ez-Fit Enzyme kinetics software (Perrella Scientific Inc. Amherst, USA). Data was expressed as Mean ± SEM, n = 3.

4.8. Cell viability assay

Cell viability assays were carried out essentially as mentioned earlier by our group using blood mononuclear cells (MNCs) by taking samples from healthy volunteers [36–38,48].

4.9. Computational approach

4.9.1. Molecular docking

In current study, molecular docking analysis was used on the synthesized oxadiazole derivatives to predict inhibitory mechanism. The study was carried out as discussed in our previous publications [48,49]. The Crystal structure of the selected target, i.e., LOX from soyabean (*Glycine* max, PDB id: 3pzw, 1.4 Å) was selected from protein data bank and used for further analysis. For the preparation of various 1,3,4-oxadiazole derivatives (**6a-o**), force field MMFF94x with RMSD gradient of > 0.01 kcal/mol/Å was used for energy minimization of compounds. The charges were assigned and hydrogen atoms were added to all the compounds and after the preparation of both ligands and protein, MOE site finder function was used to determine the binding site as discussed earlier. At the end, the 3D and 2D poses were generated and further analysed by using MOE programme [50].

4.9.2. Density functional theory calculations

In this study we have reported the HOMO and LUMO analysis of the 1,3,4-oxadiazole derivatives (**6a-o**), using the software Gaussian 09 by DFT/B3LYP calculation setup with basic set 3-21G. The output files from Gaussian 09 were viewed by Gauss view 06 software [49,51]. DFT calculations facilitated in determining the molecular properties such as energy and optimized geometry as discussed previously [52,53].

Declaration of Competing Interest

The authors declare that they have no known competing financial interests or personal relationships that could have appeared to influence the work reported in this paper.

Data availability

Data will be made available on request.

Acknowledgements

Prof. N. Riaz is thankful to Prof. Dr. Harald Gross, Institute of Pharmaceutical Biology, University of Tuebingen, Tuebingen, Germany for providing NMR and Mass analysis facility.

References

[1] A. Dick, S. Cocklin, Bioisosteric replacement as a tool in anti-HIV drug design, Pharmaceuticals 13 (2020) 36.
[2] R.H. Abd El-Hameed, S. Mahgoub, H.M. El-Shanbaky, M.S. Mohamed, S.A. Ali, Utility of novel 2-furanones in synthesis of other heterocyclic compounds having anti-inflammatory activity with dual COX-2/LOX inhibition, J. Enz. Inhib. Med. Chem. 36 (1) (2021) 977–986.
[3] S. Iranpour, A.K.M. Mosawi, A.R. Bahrami, H. Sadeghian, M.M. Matin, Investigating the effects of two novel 4-MMPB analogs as potent lipoxygenase inhibitors for prostate cancer treatment, J. Biol. Res.-Thessaloniki 28 (2021) 1–15.
[4] R. Suardíaz, L. Masgrau, J.M. Lluch, A.G. Lafont, On the regio- and stereospecificity of arachidonic acid peroxidation catalyzed by mammalian 15-lipoxygenases, a combined molecular dynamics and QM/MM study, Chem. Phy. Chem. 14 (2013) 3777–3787.
[5] H. Sadeghian, A. Jabbari, 15-Lipoxygenase inhibitors, a patent review, Expert Opinion Ther. Pat. 26 (1) (2016) 65–88.
[6] A.M. Ghanim, S. Rezq, T.S. Ibrahim, D.G. Romero, H. Kothayer, Novel 1,2,4-triazine-quinoline hybrids: the privileged scaffolds as potent multi-target inhibitors of LPS-induced inflammatory response via dual COX-2 and 15-LOX inhibition, Eur. J. Med. Chem. 219 (2021), 113457.
[7] Aziz-ur-Rehman, A. Fatima, M.A. Abbasi, S. Rasool, A. Malik, M. Ashraf, I. Ahmad, S.A. Ejaz, Ejaz, Synthesis of new N-(5-chloro-2-methoxyphenyl)-4-(5-substituted-1,3,4-oxadiazol-2-ylthio)butanamide derivatives as suitable lipoxygenase inhibitors, J. Saudi Chem. Soc. 20 (2016) S488–S494.
[8] M. Loncaric, I. Strelec, T. Moslavac, D. Subaric, V. Pavic, M. Molnar, Lipoxygenase inhibition by plant extracts, Biomolecules 11 (2021) 11020152.
[9] S.A. Ali, S.M. Awad, A.M. Said, S. Mahgoub, H. Taha, N.M. Ahmed, Design, synthesis, molecular modelling and biological evaluation of novel 3-(2-naphthyl)-1-phenyl-1H-pyrazole derivatives as potent antioxidants and 15-lipoxygenase inhibitors, J. Enz. Inhib. Med. Chem. 35 (1) (2020) 847–863.
[10] S. Zerangnasrabad, A. Jabbari, E.K. Moghadam, H. Sadeghian, S.M. Seyedi, Design, synthesis, and structure-activity relationship study of *o*-prenylated 3-acetylcoumarins as potent inhibitors of soybean 15-lipoxygenase, Drug Dev. Res. 82 (2021) 826–834.
[11] S. Tahlan, S. Kumar, B. Narasimhan, Pharmacological significance of heterocyclic 1H-benzimidazole scaffolds: a review, Bio. Med. Cent. Chem. 13 (2019) 1–21.
[12] M. Henary, C. Kananda, L. Rotolo, B. Savino, E.A. Owens, G. Cravotto, Benefits and applications of microwave-assisted synthesis of nitrogen containing heterocycles in medicinal chemistry, Royal Soc. Chem. 10 (2020) 14170–14197.
[13] M.M. Heravi, V. Zadsirjan, Prescribed drugs containing nitrogen heterocycles, Royal Soc. Chem. 10 (2020) 44247–44311.
[14] A.A. Voronin, I.V. Fedyanin, A.M. Churakov, A.N. Pivkina, N.V. Muravyev, Y. A. Strelenko, M.S. Klenov, D.B. Lempert, V.A. Tartakovsky, 4H-[1,2,3]Triazolo [4,5-c][1,2,5]oxadiazole 5-oxide and its salts: promising multipurpose energetic materials, ACS App. Ener. Mat. 3 (9) (2020) 9401–9407.
[15] M.D. Delost, D.T. Smith, B.J. Anderson, J.T. Njardarson, From oxiranes to oligomers: architectures of US FDA approved pharmaceuticals containing oxygen heterocycles, J. Med. Chem. 61 (2018) 10996–11020.
[16] M.S. Najare, M.K. Patil, M. Garbhagudi, M. Yaseen, S.R. Inamdar, I.A.M. Khazi, Design, synthesis and characterization of π-conjugated 2,5-diphenylsubstituted-1,3,4-oxadiazole-based D-π-A-π'-D′ form of efficient deep blue functional materials: photophysical properties and fluorescence "turn-off" chemsensors approach, J. Mol. Liq. 328 (2021), 115443.
[17] C. Verma, K.Y. Rhee, M.A. Quraishi, E.E. Ebenso, Pyridine based N-heterocyclic compounds as aqueous phase corrosion inhibitors: a review, J. Taiwan Inst. Chem. Eng. 117 (2020) 265–277.
[18] C.E. Stecoza, G.M. Nitulescu, C. Draghici, M.T. Caproiu, O.T. Olaru, M. Bostan, M. Mihaila, Synthesis and anticancer evaluation of new 1,3,4-oxadiazole derivatives, Pharmaceuticals 14 (2021) 14050438.
[19] J. Ma, A.K. Chinnam, G. Cheng, H. Yang, J. Zhang, J.N.M. Shreeve, 1,3,4-Oxadiazole bridges: a strategy to improve energetics at the molecular level, Ang. Chem. Int. Ed. 60 (2021) 5497–5504.
[20] V. Karabelyov, M. Kondeva-Burdina, V.T. Angelova, Synthetic approaches to unsymmetrical 2,5-disubstituted 1,3,4-oxadiazoles and their MAO-B inhibitory activity, Bio. Med. Chem. 29 (2021), 115888.
[21] J. Wang, M.F. Ansari, C.H. Zhou, Unique para-aminobenzenesulfonyl oxadiazoles as novel structural potential membrane active antibacterial agents towards drug-resistant methicillin resistant *Staphylococcus aureus*, Bio. Med. Chem. Lett. 41 (2021), 127995.
[22] A. Vaidya, D. Pathak, K. Shah, 1,3,4-Oxadiazole and its derivatives: a review on recent progress in anticancer activities, Chem. Biol. Drug Des. 97 (2021) 572–591.
[23] A.E.E. Mansouri, A. Oubella, A. Mehdi, M.Y. Aitltto, H.M.Z. Morjani, H.B. Lazrek, Design, synthesis, biological evaluation and molecular docking of new 1,3,4-oxadiazole homonucleosides and their double-headed analogs as antitumor agents, Bioorg. Chem. 108 (2021), 104558.
[24] W.A. Souza, D. Almeida, A.M. Pivatto, M. Almeida, M.V. Guedes, G.P. Resende, W. Guerra, Crystal structure and spectroscopy properties of new Pt II complexes

containing 5-alkyl-1,3,4-oxadiazol-2-thione derivatives, J. Mol. Str. 1226 (2021), 129250.
[25] Z. Yang, P. Li, Y. He, J. Luo, J. Zhou, Y. Wu, L. Chen, Design, synthesis, and biological evaluation of novel pyrethrin derivatives containing 1,3,4-oxadiazole and thioether moieties as active insecticidal agents, Chem. Pap. 74 (5) (2020) 1621–1632.
[26] M.P. Tantak, M. Malik, L. Klingler, Z. Olson, A. Kumar, R. Sadana, D. Kumar, Indolyl-α-keto-1,3,4-oxadiazoles: synthesis, anti-cell proliferation activity, and inhibition of tubulin polymerization, Bioorg. Med. Chem. Lett. 37 (2021), 127842.
[27] S. Triloknadh, C.V. Rao, B. Nagaraju, H. Balaji, M. Balaji, Design and synthesis of novel 1,3,4-oxadiazole and 1,2,4-triazolo[3,4-b]1,3,4-thiadiazole derivatives and their antimicrobial studies, Eur. J. Bio. 5 (2018) 575–587.
[28] A.T.B. Telehoiu, D.C. Nuța, M.T. Caproiu, F. Dumitrascu, I. Zarafu, P. Ioniță, C. Limban, Design, synthesis and *in vitro* characterization of novel antimicrobial agents based on 6-chloro-9H-carbazol derivatives and 1,3,4-oxadiazole scaffolds, Molecules 25 (2020) 1–18.
[29] R. Mirzazadeh, M.S. Asgari, E. Barzegari, K. Pedrood, M. Khanaposhtani, M. Sherafati, I. Gulçin, New quinoxalin-1,3,4-oxadiazole derivatives: synthesis, characterization, *in vitro* biological evaluations, and molecular modeling studies, Arch. Pharm. 2 (2021), 000471.
[30] P.K. Choubey, A. Tripathi, M.K. Tripathi, A. Seth, S.K. Shrivastava, Design, synthesis, and evaluation of N-benzylpyrrolidine and 1,3,4-oxadiazole as multitargeted hybrids for the treatment of Alzheimer's disease, Bioorg. Chem. 111 (2021), 104922.
[31] M.M. Alam, A.S. Almalki, T. Neamatallah, N.M. Ali, A.M. Malebari, S. Nazreen, Synthesis of new 1,3,4-oxadiazole-incorporated 1,2,3-triazole moieties as potential anticancer agents targeting thymidylate synthase and their docking studies, Pharmaceuticals 13 (2020) 13110390.
[32] F. Abedinifar, M.M. Khanaposhtani, N. Asemanipoor, S. Mojtabavi, M. A. Faramarzi, M. Mahdavi, M.H. Hajimiri, Synthesis and biological evaluation of a new series of benzofuran-1,3,4-oxadiazole containing 1,2,3-triazole-acetamides as potential α-glucosidase inhibitors, J. Biomol. Toxi. 35 (2021) 22688.
[33] M. Alomari, M. Taha, F. Rahim, M. Selvaraj, N. Iqbal, S. Chigurupati, K.M. Khan, Synthesis of indole-based-thiadiazole derivatives as a potent inhibitor of α-glucosidase enzyme along with *in silico* study, Bioorg. Chem. 108 (2021), 104638.
[34] N. Javid, R. Munir, F. Chaudhry, A. Imran, S. Zaib, A. Muzaffar, J. Iqbal, Exploiting oxadiazole-sulfonamide hybrids as new structural leads to combat diabetic complications via aldose reductase inhibition, Bioorg. Chem. 99 (2020), 103852.
[35] H.A. Hofny, M.F. Mohamed, H.A. Gomaa, S.A. Aziz, B.G. Youssif, N.A. Koussi, A. S. Aboraia, Design, synthesis, and antibacterial evaluation of new quinoline-1,3,4-oxadiazole and quinoline-1,2,4-triazole hybrids as potential inhibitors of DNA gyrase and topoisomerase IV, Bioorg. Chem. 112 (2021), 104920.
[36] S. Muzaffar, W. Shahid, M. Saleem, M. Ashraf, Aziz-ur-Rehman, B. Bashir, M. Ali, M. Al-Rashida, B. Baral, K. Bhattarai, N. Riaz, Evaluation of ethylated phenylcarbamoylazinane-1,2,4-triazole amides derivatives as 15-lipoxygenase inhibitors together with cytotoxic, ADME and molecular modeling studies, ChemSelect 5 (44) (2020) 14210–14216.
[37] W. Shahid, M. Ashraf, M. Saleem, B. Bashir, S. Muzaffar, M. Ali, A. Kaleem, Aziz-ur-Rehman, H. Amjad, K. Bhattarai, N. Riaz, Exploring phenylcarbamoylazinane-1, 2,4-triazole thioethers as lipoxygenase inhibitors supported with *in vitro*, *in silico* and cytotoxic studies, Bioorg. Chem. 115 (2021) 105261.
[38] S. Muzaffar, W. Shahid, N. Riaz, M. Saleem, M. Ashraf, Aziz-ur-Rehman, B. Bashir, A. Kaleem, M. al-Rashida, B. Baral, K. Bhattarai, H. Gross, Probing phenylcarbamoylazinane-1,2,4-triazole amides derivatives as lipoxygenase inhibitors along with cytotoxic, ADME and molecular docking studies, Bioorg. Chem. 107 (2021) 104525.
[39] K. Nafeesa, A.-u. Rehman, M.A. Abbasi, K.M. Khan, I. Ahmed, S. Hassan, Preliminary structure-activity relationship studies on some novel s-substituted aliphatic analogues of 5-{1-[(4-chlorophenyl)sulfonyl]-3-piperidinyl}-1,3,4-oxadiazol-2-ylsulfide, Trop. J. Pharm. Res. 15 (7) (2016) 1507.
[40] M. Akhter, N. Akhter, M.M. Alam, M.S. Zaman, R. Saha, A. Kumar, Synthesis and biological evaluation of 2,5-disubstituted 1,3,4-oxadiazole derivatives with both COX and LOX inhibitory activity, J. Enz. Inhib. Med. Chem. 26 (6) (2011) 767–776.
[41] M.A. Abbasi, ADNAN Akhtar, Aziz-ur-rehman, KHADIJA Nafeesa, S.Z. Siddiqui, K. M. Khan, MUHAMMAD Ashraf, S.A. Ejaz, Synthesis, structural characterization and enzyme inhibition studies on 5-(2-nitrostyryl)-1,3,4-oxadiazole-2-thiol derivatives, J. Chilean Chem. Soc. 58 (4) (2013) 2186–2190.
[42] B.G. Youssif, M.F. Mohamed, M.M. Al-Sanea, A.H. Moustafa, A.A. Abdelhamid, H. A. Gomaa, Novel aryl carboximidamide and 3-aryl-1,2,4-oxadiazole analogues of naproxen as dual selective COX-2/15-LOX inhibitors: Design, synthesis and docking studies, Bioorg. Chem. 85 (2019) 577–584.
[43] B. Bashir, W. Shahid, M. Ashraf, M. Saleem, S. Aziz-ur-Rehman, M. Muzaffar, H. Imran, K. Amjad, N.R. Bhattarai, Identification of phenylcarbamoylazinane-1,3,4-oxadiazole amides as lipoxygenase inhibitors with expression analysis and computational studies, Bioorg. Chem. 115 (2021), 105243.
[44] C.A. Lipinski, F. Lombardo, B.W. Dominy, P.J. Feeney, Experimental and computational approaches to estimate solubility and permeability in drug discovery and development settings, Adv. Drug Del. Rev. 23 (1-3) (1997) 3–25.
[45] D.F. Veber, S.R. Johnson, H.-Y. Cheng, B.R. Smith, K.W. Ward, K.D. Kopple, Molecular properties that influence the oral bioavailability of drug candidates, J. Med. Chem. 45 (12) (2002) 2615–2623.
[46] M.J. Waring, Lipophilicity in drug discovery, Expert Opin. Drug Discov. 5 (3) (2010) 235–248.
[47] Y. Kondo, Y. Kawai, T. Miyazawa, H. Matsui, J. Mizutani, An assay for lipoxygenase activity by chemiluminescence, Biosci. Biotech. Biochem. 58 (2) (1994) 421–422.
[48] M. Solangi, K.M. Khan, F. Saleem, S. Hameed, J. Iqbal, Z. Shafique, U. Qureshi, Z. Ul-Haq, M. Taha, S. Perveen, Indole acrylonitriles as potential anti-hyperglycemic agents: synthesis, α-glucosidase inhibitory activity and molecular docking studies, Bioorg. Med. Chem. 28 (2020), 115605.
[49] M.J. Frisch, G.W. Trucks, H.B. Schlegel, G.E. Scuseria, M.A. Robb, J.R. Cheeseman, G. Scalmani, V. Barone, B. Mennucci, G.A. Petersson, H. Nakatsuji, M. Caricato, X. Li, H.P. Hratchian, A.F. Izmaylov, J. Bloino, G. Zheng, J.L. Sonnenberg, M. Hada, M. Ehara, K.Toyota, R. Fukuda, J. Hasegawa, M. Ishida, T. Nakajima, Y. Honda, O. Kitao, H. Nakai, T. Vreven, J.A. Montgomery Jr., J.E. Peralta, F. Ogliaro, M.J. Bearpark, J. Heyd, E.N. Brothers, K.N. Kudin, V.N. Staroverov, R. Kobayashi, J. Normand, K. Raghavachari, A.P. Rendell, J.C. Burant, S.S. Iyengar, J. Tomasi, M. Cossi, N. Rega, N.J. Millam, M. Klene, J.E. Knox, J.B. Cross, V. Bakken, C. Adamo, J. Jaramillo, R. Gomperts, R.E. Stratmann, O. Yazyev, A.J. Austin, R. Cammi, C. Pomelli, J.W. Ochterski, R.L. Martin, K. Morokuma, V.G. Zakrzewski, G.A. Voth, P. Salvador, J.J. Dannenberg, S. Dapprich, A.D. Daniels, O. Farkas, J.B. Foresman, J. V. Ortiz, J. Cioslowski, D.J. Fox, Gaussian 09 (D01), Inc., Wallingford, CT, USA (2010).
[50] MOE, Molecular operating environment (MOE), 2014.09; Chemical computing group Inc., 1010 Sherbooke St. West, Montreal, QC, Canada, 2014 (2016).
[51] GaussView version 5 K.R. Dennington, T. Keith, J. Millam-Semichem Inc., Shawnee Mission, GaussView (2009) version 5.
[52] W. Shahid, S.A. Ejaz, M. al-Rashida, M. Saleem, M. Ahmed, J. Rahman, N. Riaz, M. Ashraf, Identification of NSAIDs as lipoxygenase inhibitors through highly sensitive chemiluminescence method, expression analysis in mononuclear cells and computational studies, Bioorg. Chem. 110 (2021) 104818.
[53] T. Lu, F. Chen, Multiwfn: A multifunctional wavefunction analyzer, J. Comp. Chem. 33 (2012) 580–592.